

# Studies on Variation of Drag Coefficient for Flow past Cylindrical Bodies Using ANSYS

*A Thesis Submitted in Partial Fulfillment of the Requirements for the Degree of*

**Master of Technology  
In  
Civil Engineering**



**ANTA MURMU**

**DEPARTMENT OF CIVIL ENGINEERING  
NATIONAL INSTITUTE OF TECHNOLOGY, ROURKELA**

**2015**

# **Studies on Variation of Drag Coefficient for Flow past Cylindrical Bodies Using ANSYS**

*A Thesis Submitted in Partial Fulfillment of the Requirements for the  
Degree of*

*Master of Technology  
in  
Civil Engineering*

WITH SPECIALIZATION IN  
WATER RESOURCES ENGINEERING

**Under the guidance and supervision of**  
Prof Awadhesh Kumar

*Submitted By:*

**ANTA MURMU  
(ROLL NO. 213CE4105)**



**DEPARTMENT OF CIVIL ENGINEERING  
NATIONAL INSTITUTE OF TECHNOLOGY, ROURKELA  
2015**



**National Institute of Technology**

**Rourkela**

## ***CERTIFICATE***

This is to certify that the thesis entitled “*STUDIES ON VARIATION OF DRAG COEFFICIENT FOR FLOW PAST CYLINDRICAL BODIES USING ANSYS*” being submitted by **ANTA MURMU** in partial fulfilment of the requirement for the award of *MASTER OF TECHNOLOGY* Degree in *CIVIL ENGINEERING* with specialization in *Water Resources Engineering* at National Institute of Technology Rourkela, is an authentic work carried out by him under my guidance and supervision.

To the best of my knowledge, the matter embodied in this Project Report has not been submitted to any other University/Institute for the award of any Degree/Diploma.

**Prof. Awadhesh Kumar**

Department of Civil Engineering

National Institute of Technology,

Rourkela, Odisha.

Place:Rourkela

Date:

## **ACKNOWLEDGEMENTS**

I consider the completion of this research as dedication and support of a group of people rather than my individual effort. I wish to express gratitude to everyone who assisted me to fulfill this work.

First and foremost I offer my sincerest gratitude to my supervisor, Dr. Awadhesh Kumar, who has supported me throughout my thesis with his patience and knowledge while allowing me the room to work in my own way. I attribute the level of my Master's degree to his encouragement and effort and without him this thesis, too, would not have been completed or written. One simply could not wish for a better or friendlier supervisor.

I am very grateful to all other faculty members for their helpful suggestions during my entire course work and the Head of the Department of Civil Engineering and Dean SRICCE of NIT Rourkela for providing all the facilities specially the library and the books that needed for this project work.

I also wish to extend my thanks to all my friends Arunima, Deepika, Sumit, Rajender, Sanoj and Ranjit who really helped me in every possible way they could.

Last but certainly not least, I would like to express my gratitude to my parents for their encouragement. The goal of obtaining a Master's degree is a long term commitment, and their patience and moral support have seen me through to the end.

Date:

(Anta Murmu)

## Table of Contents

	List of Figures	v
	List of Tables	vii
	List of Notations	viii
	ABSTRACT	ix
1	<b>CHAPTER I</b> <b>INTRODUCTION</b>	
	1.1 General	1
	1.2 Fluid dynamics	1
	1.2.1 Aerodynamics	1
	1.2.2 Hydrodynamic	2
	1.3 Flow classification	2
	1.3.1 Uniform and Non-uniform Flow	2
	1.3.2 Compressible and Incompressible	3
	1.3.3 Steady and Unsteady Flow	3
	1.3.4 Laminar, Transient and Turbulent Flow	4
	1.3.5 Sub-sonic, Sonic, Super-sonic flow	4
	1.4 Drag Force	4
	1.4.1 Drag force Expression	4
	1.4.2 Coefficient of Drag	5
	1.5 Numerical Modelling	5
	1.5.1 Pre-processing	6
	1.5.2 Solver	6
	1.5.3 Post-processing	6
	1.6 Importance and Objective of The Research	7
	1.7 Organisation of Thesis	8
2	<b>CHAPTER 2</b> <b>LITERATURE STUDY</b>	
	2.1 GENERAL	10
	2.2 Pre-Study on Numerical Analysis	10
	2.3 Variation Of Drag Coefficient For Different Range Of Reynolds Number	13
	2. 4 Reduction of Drag For a Circular Cylinder	16
	2.5 Pre-Research and Experimentation Done on Bluff Bodies And Their Drag Coefficient	18
	2.5.1 Cylindrical Bodies	19
	2.6 Surface Roughening Of Cylindrical Bodies	19
	2.7 Distribution Of Pressure	20
3	<b>CHAPTER 3</b> <b>COMPUTATIONAL MODELLING</b>	
	3.1. General	22
	3.2. Governing Equation And Numerical Models For CFD	22
	3.3. Governing Equation	22
	3.3.1 Continuity Equation	24
	3.3.2 Momentum Equation	24
	3.4. Design of Turbulence Models	24
	3.4.1 List of models	24
	3.5. Discretization Technique	27
	3.5.1 Finite Difference Method	27
	3.5.2 Finite Volume Method	27

	3.5.3 Pressure-Velocity coupling	28
4	CHAPTER 4	
	NUMERICAL ANALYSIS	
	4.1 Methodology	29
	4.1.1 Pre-Processing	29
	4.1.1(a) Creation of Model and Domain	29
	4.1.1(b) Generation of Mesh for the Domain	30
	4.1.2 Solver modelling for the Domain	32
	4.1.3 Post-Processing	33
	4.2 Physical Setup For The Study Area	33
	4.2.1 Boundary and Cell Zone Condition	34
	4.3. Turbulence solution	35
5	CHAPTER 5	
	EXPERIMENTATION	
	5.1 General	36
	5.2 Equipment used	36
	5.3 Experiment Method and Procedure	37
	5.3.1 Pressure Distribution Technique	38
6	CHAPTER 6	
	DISCUSSION OF RESULTS	
	6.1 General	40
	6.2 Numerical Results	40
	6.2.1 Flow velocity	40
	6.2.2 Size of the cylinder	41
	6.2.3 Surface Roughness	42
	6.2.4 Reynolds Number and water as the fluid	45
	6.2.5 Contour	48
	6.3 Experiment Results	52
	6.4 Development of Correlation	54
7	CHAPTER 7	
	CONCLUSIONS AND FUTURE SCOPE	
	7.1 General	59
	7.2 Drag Force	59
	7.3 Scope of the Study	60
	REFERENCES	61

## LIST OF FIGURES

Fig. No.	Description	Page No.
1.1	Forces on Aerofoil	1
1.2	Drag Force on The Cylinder	5
3.1	Conservation of Mass in 2-D Domain	24
3.2	Structured Mesh For Finite Volume Method	29
4.1	Replication of Apparatus Into ANSYS Geometry Model	31
4.2	Computational Fluid Domain	31
4.3	Tetrahedral Mesh of Domain	32
4.4	Solver Selection	34
4.5	Choosing of Pressure-Velocity Coupling	34
4.6	Flow Domain	35
5.1	Smooth cylinder	36
5.2	Cylinder of varying roughness	36
5.3	Cylinders fitted to circular disc with angular calibrations	37
5.4	Schematic picture of Airflow bench	38
5.5	Pressure Measurement Setup	38
5.6	Pressure Distribution Method	39
6.1	Drag force on cylinder of different radius	40
6.2	Variation of Drag Force Due To Change in Area	41
6.3	Variation of Drag Force with Varying Length of the Cylinder	42
6.4	Different Roughness with varying Velocity.	42
6.5	Effect of roughness for R=6.25mm	43
6.6	Effect of roughness for R=7.5mm	43
6.7	Effect of roughness for R=10mm	44
6.8	Effect of roughness for R=12.5mm	44
6.9	Drag $V_s$ Reynolds No. for R=10mm	45
6.10	Drag $V_s$ Reynolds No. for R=12.5mm	45
6.11	Coefficient of Drag $V_s$ Reynolds No. for R=7.5mm; $k_s=0\mu\text{m}$	46
6.12	Coefficient of Drag $V_s$ Reynolds No. for R=7.5mm; $k_s=348\mu\text{m}$	46
6.13	Coefficient of Drag $V_s$ Reynolds No. for R=7.5mm; $k_s=265\mu\text{m}$	47

6.14	Coefficient of Drag $V_s$ Reynolds No. for $R=7.5\text{mm}$ ; $k_s=165\mu\text{m}$	47
6.15	Pressure Contour for $R=6.25\text{mm}$	48
6.16	Pressure Contour for $R=7.5\text{mm}$	48
6.17	Pressure Contour for $R=10\text{mm}$	49
6.18	Pressure Contour for $R=12.5\text{mm}$	49
6.19	Velocity Contour for $R=6.25\text{mm}$	49
6.20	Velocity Contour for $R=7.5\text{mm}$	50
6.21	Velocity Contour for $R=10\text{mm}$	50
6.22	Velocity Contour for $R=12.5\text{mm}$	50
6.23	Velocity Vector for $R=6.25\text{mm}$	51
6.24	Velocity Vector for $R=7.5\text{mm}$	51
6.25	(a) Close View of Velocity Vector around the Cylinder; (B) Velocity Profile and (C) Flow Separation	52
6.26	Pressure coefficient for $R=7.5\text{mm}$ ; $k=348\mu\text{m}$	53
6.27	Pressure coefficient for $R=7.5\text{mm}$ ; $k=265\mu\text{m}$	53
6.28	Drag force against varying roughness	54
6.29	Drag force against varying roughness	55
6.30	Drag force against varying roughness	55
6.31	The relationship between Drag force and $x$	56
6.32	Final correlation	56
6.33	Comparison plot for varying Velocity	57
6.34	Comparison plot for varying Diameter	57
6.35	Comparison plot for varying Roughness	58



***LIST OF TABLES***

<b>Table no.</b>	<b>Description</b>	<b>Page no.</b>
3.1	Turbulence Model	25
4.1	Mesh Quality	31
5.1	Detail Of Geometric Parameter	37

## List of Notations

$A$	Projected area
$C_D$	Drag coefficient
$C_f$	Skin friction coefficient
$C_P$	Pressure coefficient
$D$	Diameter of cylinder
$F_D$	Drag force
$K_s$	Roughness
$L$	Length of cylinder
$M$	Mass
$P_s$	surface pressure
$p_0$	Static pressure
$P$	Total pressure
$R$	Gas constant
$Re$	Reynolds Number
$R^2$	Regression coefficient
$T$	Time
$U$	Uniform Speed
$V$	Velocity
$X$	Independent Variable
$\nu$	Kinematic viscosity
$\mu$	Dynamic viscosity
$\rho$	Density
$\tau$	Shear stress
$\Theta$	Angle of incidence in degree

# ABSTRACT

The fluid in motion exerts a force on the solid body immersed in it or the solid body moving in a fluid resulting the force exerted on the solid by the fluid such as flow around an airplane, the drag force acting on automobile, trees and underwater pipelines. The Drag Force is the function of drag co-efficient which is mainly depended on the flow velocity, surface body roughness, body orientation immersed in the fluid with the direction of fluid flow and the object configuration i.e. shape and size of the object. Literature review speaks about the different shape and size of the cylinder that had been taken for the study of drag force over the cylindrical bodies. The selected shape of the cylinder that had been used for experimentation are circular cylinder, wavy cylinder, and the square shape cylinder. These all investigation over the different shape of cylinder give us quite explanation about the dependency of drag force on the cylinder and its shape by the flowing fluid with its qualitative and quantitative conclusion. However the duration of carrying these experiment is more and consuming space for large wind tunnel with constant voltage power supply to maintain the flowing velocity. The change in the power supply causes change in the flow velocity resulting error in the drag force calculation. Some literature shows numerical approach use of software like ANSYS Fluent, CFX, etc. for the calculation of drag force over body in a flowing fluid with more effective and efficient. The application of software provides opportunity for desirable change in the shape and size, surface roughness of the test object or body without extra cost or no more of new model for the experiment.

The present work is the advancement of Researcher with their research to the growing digital world. The paper shows the importance of the software and its effective work in the field of research. Thesis involves the experimentation and numerical approach for calculation of drag force over the circular cylinder of different length, different diameter and different surface roughness for different range of flow velocity. The experimentation is carried out on the Air flow bench (AF12), with the application of direct weighing method, pressure distribution method, the co-efficient of drag is obtained and for the numerical approach the ANSYS Fluent software is used for the simulation. Numerical method involve the application of Computational Fluid Dynamics (CFD). CFD follows the computational code based on Navier-Stokes equation to solve the fluid flow problem, providing satisfactory result with significant cost reduction in comparison to the experiment model. The turbulence model, k- $\epsilon$  model and Finite Volume Method (FVM) with SIMPLE spatial discretization method of second order

correction is used for the calculation of drag force over the circular cylinder of varying diameter and varying length and varying surface roughness .

Drag force, co-efficient of drag resulted for varying diameter, surface roughness of the circular cylinder is noted and a comparison graph has been plotted between experimental and numerical result. The comparison shows the numerically predicted data to be within the acceptable error range of 15% which is comparatively less than the error range of 20% as per the literature. After validating the numerical results, the numerical model was run again taking the liquid water as the flowing fluid and results obtained are shown.

Keywords: *Computational Fluid Dynamics, Finite Volume Method, ANSYS Fluent, Discretization, Drag Force, Coefficient*

# CHAPTER 1

## INTRODUCTION

---

### 1.1.GENERAL

In our daily living world, the solid bodies are repeatedly subjected to fluid flow, such as the flow of air over buildings, trees resulting drag force on it and on automobiles. The underwater flow like submarines; flow of fluid in pipes; flying of birds and jets are due to lift generated by fluid flow. The drag produce by the heavy wind flow like storm causing toppling of trees, house, vehicle and also reduction automobile speed, high consumption of fuel; generation of noise and vibration in solid bodies due to flowing fluid. Therefore, it is important to understand the fluid flow properties and the drag force exerted on the bodies submerged in it, which helps us to develop certain model to study the forces acting on the body that can reduce the drag resulting in high speed, less fuel consumption, stability of the building, bridges and reduction in head loss in pipe flow.

### 1.2.Fluid Dynamics

Fluid Dynamics is the branch of science that deals with the flow of fluid (i.e. liquids and gases) or fluid in motion. It is one part of the fluid mechanics and other part is the fluid statics, which deals with the fluid at rest. Fluid Dynamics is subdivided into aerodynamics and hydrodynamics.

#### 1.2.1 Aerodynamics

Aerodynamics is the study that deals with the gases in motion. The study involves the calculation of forces around the solid body in the flow field. The main force that are acting on the body are Drag force, Lift force, Weight of the body and thrust.

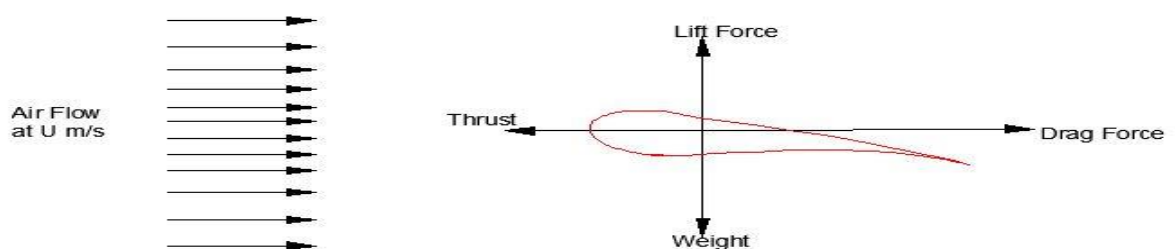


Fig: 1.1.Forces on Aerofoil

Drag force affects the speed and fuel consumption for the most of automobiles. Therefore to achieve higher speed with low fuel consumption drag force must be reduce either by streamlining the bodies or by giving the smooth contour in front of the vehicle (Gorsche, 2001).

### 1.2.2 Hydrodynamics

Hydrodynamic deals with the liquid (generally water) in motion and the forces acting on it. It includes the calculation of properties like density, flow velocity, pressure.

Flow velocity is the free stream velocity i.e. the fluid velocity that's approaching the body immersed in it. It is denoted as  $U_s$  or  $V$ . when flow is along x-axis it is symbolize as 'u' because u represent the x-component. For the convenience flow velocity is assumed to be uniform and steady.

### 1.3 Flow Classification

The grouping or categorising of Fluid flow in given class with respect to flow speed, fluid properties in the flow field with time and space and with given constant like Reynolds number(Re), Mach number is termed as the flow classification. The flow of fluids are classified as Uniform and Non-uniform flow, Compressible and Incompressible flow, Steady and Unsteady flow, Laminar flow, Transient flow, Turbulent flow, subsonic flow, Supersonic flow, transonic flow, hypersonic flow and different flow regimes.

#### 1.3.1 Uniform and Non-uniform Flow

Flow is said to be Uniform, when the velocity of flow remain constant at any given time along the length of direction of flow (i.e. with space).

Mathematically,

$$\left(\frac{\partial V}{\partial s}\right)_{t=constant} = 0$$

Where  $\partial V$  = change of velocity

$\partial s$  = length of flow in the direction S

Non-uniform Flow is the flow of fluid in which the velocity varies at any given time with the space.

Mathematically,

$$\left(\frac{\partial V}{\partial s}\right)_{t=constant} \neq 0$$

### 1.3.2 Compressible and Incompressible

Flow of fluid in which fluid density varies from point to point is said to be Compressible Flow.

$$\rho \neq \text{constant}$$

Incompressible Flow is the flow where density of the fluid is constant throughout the flow.

$$\rho = \text{constant}$$

### 1.3.3 Steady and Unsteady Flow

The kind of flow where the fluid properties like density, pressure, velocity, etc. at a point does not vary with time.

Mathematically,

$$\left(\frac{\partial V}{\partial t}\right)_{x_0, y_0, z_0} = 0, \quad \left(\frac{\partial p}{\partial t}\right)_{x_0, y_0, z_0} = 0, \quad \left(\frac{\partial \rho}{\partial t}\right)_{x_0, y_0, z_0} = 0$$

Where  $(x_0, y_0, z_0)$  is a fixed point.

Unsteady Flow is the flow of fluid where the fluid properties change at a given point with time.

Mathematically,

$$\left(\frac{\partial V}{\partial t}\right)_{x_0, y_0, z_0} \neq 0, \quad \left(\frac{\partial p}{\partial t}\right)_{x_0, y_0, z_0} \neq 0, \quad \left(\frac{\partial \rho}{\partial t}\right)_{x_0, y_0, z_0} \neq 0$$

### 1.3.4 Laminar, Transient and Turbulent Flow

The fluid flow in which the fluid particles follow stream line path of flow, and the stream lines are parallel to each other. This kind of flow is termed to be laminar flow.

The turbulent flow is generally known by the formation of wakes or eddies behind the solid object in the flow. The fluid particles follow a zigzag flow path. Turbulent flow occurs due to the interaction of inertia and viscous term in the equation of Momentum.

The flow is categorised by the Reynolds number as follows:

When Reynolds number ( $R_e$ ) is less than 2200; the flow is said to be laminar flow.

Reynolds number more than 4000 is known to be turbulent flow.

The flow is said to be transient when the  $R_e$  value is in between 2200 and 4000.

### 1.3.5 *Sub-sonic, Sonic, Super-sonic flow*

For compressible flow Mach number a dimensionless parameter play an important role in classifying the flow. Mach number is the square root of ratio of inertia force to the elastic force or it is the ratio of velocity of fluid / body moving in fluid to the velocity of sound in the fluid. Mathematically

$$M = \frac{V}{C}$$

Where

V is the velocity of fluid

C is the velocity of sound in the fluid

A flow is known as Sub-sonic if the flow velocity is less than that of the sound i.e.  $M < 1$ .

When the velocity of the fluid equals that of the sound and Mach numbers attains the value of 1, the flow is termed as sonic flow. Super-sonic flow is the flow which velocity is more than that of the Sonic flow i.e. value of Mach number  $M > 1$ .

## 1.4 DRAG FORCE

When a body is subjected to the flowing fluid or the body is moving within the fluid, an effective opposing force is exerted on the body by the fluid, this restrictive force felt by the body is known as Drag Force. The drag force is always along the direction flowing fluid.

### 1.4.1 *Drag force Expression*

Consider the cylinder body immersed in the flowing fluid having viscosity moving along x-direction with a constant free stream velocity of U m/s. Figure 1.2 shows the forces acting on the small element of cylinder.

Where,  $P.dA$  is the pressure force acting normal to the surface;  $\tau.dA$  is the shear force acting tangential to the surface and  $\Theta$  be the angle between the x direction & force due to pressure. Therefore the drag force  $F_D$  is the summation of shear force and pressure force both along the flow direction. Mathematically, given as follows:

$$F_D = P.dA \cos \theta + \tau.dA \cos(90 - \theta) = P.dA \cos \theta + \tau.dA \sin \theta \quad \text{Eq. (1.1)}$$



$$\therefore F_D = \int P \cos \theta dA + \int \tau \sin \theta dA \quad \text{Eq. (1.2)}$$

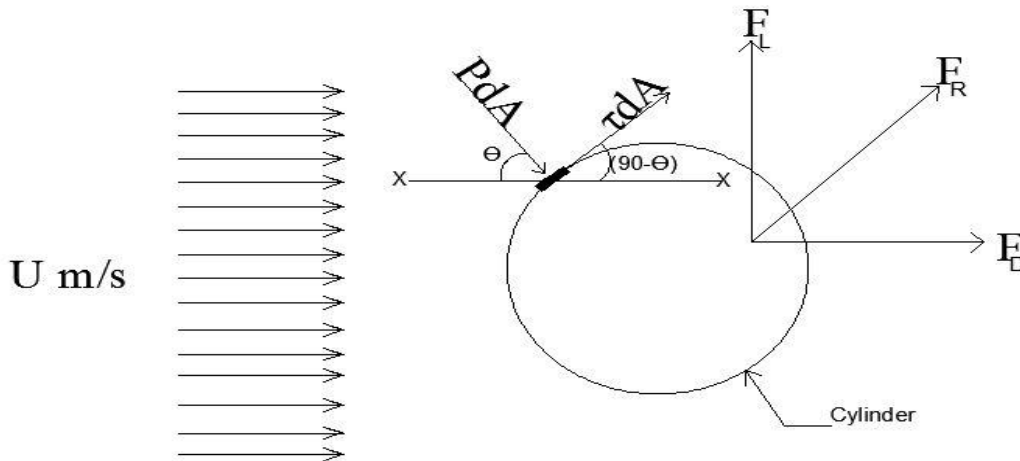


Fig. 1.2: Drag force on the Cylinder

The pressure force on the cylinder surface is also known as pressure drag or form drag and the shear force is called as skin drag or friction drag or shear drag. The total drag for the moving fluid over the stationary body can be calculated by the following equation:

$$F_D = \frac{1}{2} C_D A \rho U^2 \quad \text{Eq. (1.3)}$$

Where,  $C_D$  = coefficient of drag,

$\rho$  = fluid density,

$A$  = projected area,

$U$  = free stream velocity.

#### 1.4.2 Coefficient of Drag

The coefficient of drag is the ratio of total drag to term  $(\frac{1}{2} A \rho U^2)$ . It is dimensionless and depends on geometry of the body, stream velocity, Reynolds No. and angle of impact.

### 1.5 NUMERICAL MODELLING

In our daily life we come across many fluid flow problem which are being passed unnoticed. We travel lots from one place to other through various means of transportation like bus, trains, cars, motor-cycle, airplane, ship etc. I'm sure everyone has experienced Most of the numerical models are based on Computational Fluid Dynamics (CFD), which involve numerical methodology to solve heat transfer, fluid flow problem and chemical reaction by the means of software packages for the simulation in the computers.

CFD is a very magnificent and powerful technique with vast field of application in both industrial and non-industrial areas. The availability of user friendly graphical interface software package like ANSYS INC. and high performance computers has increased the interest among

the researchers and engineers to work on the simulation based on CFD. The technique or methodology applied by CFD can be used in various field like hydrodynamics of submarine, ships; aerodynamics of automobile, airplane; flows in rivers, channel, oceans; weather prediction; wind load over the building; diffusers; distribution of pollutants. The CFD works with the certain group of code and numerical algorithm to solve the problem associated with the fluid flow. There are three codes that the user must follow to get the desired solution. The code involves are:

- (i) Pre-processing;
- (ii) Solver;
- (iii) Post-processing

### ***1.5.1 Pre-processing***

In a CFD program it plays a role of input part or initiating part for the flow problem. There are few steps that the user must carry out which are as follows:

- Geometry formation, constituting the computational domain
- Sub-dividing the domain into small number of cells
- Applying suitable model required as per the physical phenomena
- Defining the fluid properties
- Giving boundary condition

### ***1.5.2 Solver***

The software like CFX/ANSYS, FLUENT, PHOENICS, and STAR-CD uses finite difference formulation technique which is one of the three numerical method that based on the CFD solver. The numerical technique are: Finite volume method; Finite element method and Finite Difference method. The steps that involves in the solver are

- Fluid flow governing equation are integrated over the cells of domain
- Discretization: the integral equation are converted into a algebraic equations
- Interpolation of algebraic equation is done for the solution

The complex physical phenomena and non-linear equation are solved iteratively. TDMA (tri-diagonal matrix algorithm) and SIMPLE algorithm are used to solve the algebraic equation line-by-line and to provide a good linkage between pressure and velocity.

### ***1.5.3 Post-processing***

This act as the last procedure in the CFD programing tool. It is an interesting tools of recording the results with versatile visualization technique, high graphics and operator-friendly interface.

It includes:

- Display of mesh and domain
- Contour visualization
- Plotting vectors
- Surface plot

## 1.6 Importance and Objective of the Research

The current work is focus on the drag force and drag coefficient over the cylindrical body mainly circular. Mostly drag is an unwanted force that we have to dealt with, it reduces speed of the vehicle and increases the fuel consumption, in pipe flow it decreases the flow speed and heavy winds can even disrupt the high building. Therefore it is important for us to diminish the effect of drag force or reduce it for the better speed of the automobile, safety of the buildings and have good fuel efficiency. The study explains about the factors that affects the value of drag on the circular cylinder and suggest a suitable methods to reduce it. There are two approaches that have been employed in this study to find the drag force over the cylindrical bodies and they are: Numerical and Experimentation. For the Numerical study, ANSYS FLUENT is used and pressure distribution technique for the experimentation. The calculation drag requires great concern about the parameters that it depends on like velocity of the flow, surface roughness of the body, projected area of the body i.e. length and diameter for the circular cylinder. The aim of the study are listed below:

### 1. Numerical methods:

- ✓ To find the drag force under varying free stream velocity, changing diameter and length of cylinder, taking different surface roughness.
- ✓ The visualization of pressure contour and velocity contour distribution for the flow.
- ✓ To measure the coefficient of drag for different flow velocity and Reynolds No. taking liquid water as the flowing fluid.

### 2. Experiment approach:

- ✓ Using pressure method to calculate the drag force for various flow, different diameter of the cylinder and varying roughness.
  - ✓ To measure the coefficient of pressure on cylinders for varying parameter like velocity and surface roughness.
  - ✓ To purpose a correlation for the drag force.
- ❖ Finally comparing the results obtain from the above two mentioned methods and the predicted value produced by the developed correlation.

## 1.7 Organisation of Thesis

The paper contain seven different chapters. General introductory part is provided in Chapter 1, literature review is briefly described in Chapter 2, numerical models are detailed in Chapter 3, numerical analysis and experimental works are explained in Chapter 4, the results and discussion are part of chapter 5, the correlation was being developed in chapter 6 and lastly conclusions is drawn, future scope and references are delivered in Chapter 7.

**Chapter-1** the introduction of fluid mechanics, flow classification, various nature of drag force with its effect on the drag coefficient and distribution of pressure and the aim of the research are detailed.

**Chapter-2** shows the summary of literature review as per the date-to-date research work have been carried out related to the prediction drag force either by numerical or experimental methods considering different parameter like drag coefficient, pressure coefficient, different shape and size of the body, and surface roughness.

**Chapter-3** describes the numerical model with details of governing equation: conservation of mass, momentum and energy. The various method of investigation are outlined. The parameter includes the cylinders of different radius, varying roughness and change in the free stream velocities.

**Chapter- 4** presents numerical analysis. The analysis of drag coefficient ( $C_D$ ) i.e. the ratio of drag force to  $0.5\rho Av^2$ . Thus, the coefficient of drag is a function of drag force ( $F_D$ ). The drag force is calculated by using the ANSYS model. The standard k- $\epsilon$  model is applied to get the solution. The different contour are obtained in the CFD post. The different boundary condition are used and different inlet velocity are chosen according to the experimental information. The surface roughness and fluid properties are assigned at the boundary condition.

**Chapter- 5** represent the experimentation procedure and the equipment set up. Pressure distribution technique is employed to find the coefficient pressure and then it is used to calculate the  $C_D$  over the cylinder and finally the drag force is obtained.

**Chapter -6** gives the results, plots that are being found and obtained by the use of different method described in the chapter 4 & 5. The comparison is drawn for the different results and solution. The angle is noted down where the flow get separated. The correlation is being generated by applying the dimension analysis. The drag force is expressed as:

(i) Dimensional terms:  $F_D = C(V^{n_1})(D^{n_2})(\mu^{n_3})$

(ii) Dimensionless terms:  $\frac{2F_D}{\rho AV^2} = C(R_e)^{n_1}\left(\frac{k}{D}\right)^{n_2}$



## *INTRODUCTION*

The developed correlation is used to predict the drag force over the cylindrical bodies for varying parameter involving the geometry of the cylinders and flowing fluid property. The predicted drag is compared with numerical and experimental value.

**Chapter-7** holds the summary and conclusion of the present study. It describe the characteristic of drag, and shows how drag change with change in the system parameter. Future scope of the study are outlined.

References are provided at the end of the paper.

## CHAPTER 2

### *LITERATURE STUDY*

---

#### 2.1 GENERAL

A literature covers varieties of theories and experimental studies both analytical and numerical. In this we will have a quick review that will focus on important aspect of theories that has been develop constantly in these past years. The topic contains the past research works that has been the applied for the study of science theory and for the betterment of livelihood. The study of forces acting on the solid body submerged in the fluid (air or water) is of great importance in our daily living life. A fine piece of work and great effort has been done by the researchers in the past. The combination of coefficient of pressure drag and the coefficient of friction drag form the coefficient of drag or drag coefficient. Drag coefficient is function of various factor like relative velocity of flow, relative surface roughness, shape and size of the object, orientation of the body with the flow and the properties of the fluid. The flow in pipe or the flight of a bird or plane and the speed of the moving vehicle all of these are mostly depended on the drag coefficient, such facts brought the importance and has motivated many researchers to carry out the study on the various parameter involving the pressure distribution around the body, physical properties of fluid and solid. Therefore this chapter will describe the drag force and how it varies with the geometric parameter of the body and the flow speed of the fluid.

#### 2.2 Pre-Study on Numerical Analysis

**M.N. Zakharenkov (1997)** the beginning of separated partition is considered on the premise of a numerical arrangement of the full Navier-Stokes equation. Fluxes of vortices with distinctive signs produced with double the recurrence of cylinder oscillating from the cylinder to the external surface of a confined fluid layer as concentric rings. Close to the critical layer between the connected layer and the primary flow these rings are torn and pleated to the areas of isolated vortices of the comparing sign. The type of confined isolated vortices is like that of vortices starting from a circular cylinder at rest in a uniform flow. Movement of the flow to a non-symmetric structured with Karman vortex road created at a Reynolds number (taking into account the radius) more prominent than 17 is uncovered. This critical Reynolds number is littler than that for a circular cylinder with no velocity in a stream having viscosity (where

$Re=20$  has been found as the value of critical  $Re_c$ ) and relates to the Reynolds number extrapolated from the critical value for the stationary cylinder by expanding the radius by the appended layer thickness. The flux vortices from the cylinder surface quickly into the separated area diminishes as the cylinder frequency increments with oscillation. Generation of vorticity on the exterior surface was mainly due to flow potential violation in unattached separation area.

**Guo-ping and Shih (1999)** A hybrid finite difference and vortex method (HFDV), in light of the domain decomposition method (DDM), is utilized for computing the stream around a turning circular cylinder at Reynolds number  $Re=1000, 200$  and the angular-to-rectilinear pace proportion  $\alpha=(0.5, 3.25)$  separately. A completely understood implicit equation was solved using third-order finite difference method, and the derived expansive wide band matrix was solved by an exceptionally proficient altered inadequate LU disintegration conjugate inclination system gradient (MILU-CG). The long-lasting, completely created highlights about the varieties of the vortex designs in the wake, and additionally the drag and lift constrains on the barrel, are given. The computed streamline shapes are in great concurrence with the tentatively imagined stream pictures. The presence of the basic state is affirmed once more, and the single side shed vortex design at the basic state is indicated surprisingly. Additionally, the enhanced lift-to-drag power proportion was found close the critical state.

**Mittal and Raghuvanshi (2001)** we have seen via analysts before that vortex shedding behind round cylinder can be modified, and now and again smothered, more than a constrained scope of Reynolds numbers by fitting arrangement of a second, much littler, "control" cylinder in the close wake of the principle cylinder. For such circumstances the results are displayed by the numerical calculations. The Navier–Stokes equation for incompressible flow was discretised by the application of finite element method. At a relative location of primary and control cylinder with the less Reynolds numbers, the vortex shedding from the primary chamber is totally stifled. Amazing assertion was seen between the current processing's and experimental discoveries of different scientists. With an end goal to clarify the component of control of vortex shedding, the stream wise pressure variation near the shear layer of the primary cylinder was measured and analysed for different cases, with the presence of control cylinder and without the control chamber. The shear layer is balanced by the positive pressure gradient produced by the control cylinder when the vortex shedding close to wake is smothered.

**Yan-Xing et.al (2004)** a numerical approach was performed to explore the flow impelled by a sphere moving along the axis of a rotating cylinder which was packed with the fluid having viscous. Three-dimensional incompressible Navier–Stokes mathematical statements are fathomed utilizing a finite element technique. The goal of this study is to analyse the highlight of waves produced by the Coriolis force at moderate Rossby numbers and that what exactly degree the Taylor–Proudman hypothesis is legitimate for the rotating viscous flow at low Rossby number and substantial Reynolds number. Computations have been attempted at the Rossby numbers ( $Ro$ ) of 1 and 0.02 and the Reynolds numbers ( $Re$ ) of 200 and 500. At the point when  $Ro=O(1)$ , inertia are shown in the rotating sphere. The effects of the Reynolds number and the proportion of the sphere radius and that of the revolving cylinder on the flow structure are inspected. At the point when  $Ro \ll 1$ , as anticipated by the Taylor–Proudman hypothesis for inviscid flow, the alleged 'Taylor section' is too produced in the thick fluid flow after a developmental course of vortical flow structures. The beginning development and final arrangement of the 'Taylor section' are displayed. As indicated by the present estimation, it has been verified that major hypothetical articulation about the turning flow of the inviscid fluid might still roughly foresee the turning flow structure of the viscous fluid in a certain Reynolds number regime.

**Yang and Shao (2005)** we show a drag part conspire for surfaces of different harshness densities. The aggregate drag is apportioned into three segments: a weight drag, a skin drag because of force exchange to the surfaces of rough components and a surface drag because of energy exchange to the ground surface. We present a viable frontal range record to describe the shared shielding impact of harshness components on drag segment and propose a system for the count of the drag parts. The drag segment plan is then connected to the figuring of mass amounts, for example, harshness length and zero-plane removal stature. The outcomes are contrasted and wind-tunnel estimations. Harshness length is found to increment with frontal area index  $\lambda$  to a greatest at about  $\lambda=0:2$ , and afterward diminishes with  $\lambda$ . This finding is in concurrence with perceptions. The drag segment plan has applications to concentrating on scalar trade in limit layers over unpleasant surfaces, for example, urban limit layers.

**Jones and Clarke (2008)** flow over the sphere was investigated by the application of fluent code of computational fluid dynamics for the various flows. The type of flows that are considered for the simulation of purpose are steady-state and time-dependent laminar flow for the  $Re$  value of 100 and 300 respectively, and for the flow to be turbulent Reynolds number are taken as  $10^4$  and  $10^6$ . this study shows the accuracy of code and to understand flows over



the bluff body, like submarine and other vehicles. The results are contrasted both computational and experimental and we have seen that the numerical approach on the fluid characteristic for sphere gives comparatively good result

**Niels and Zahel (2010)** This article depicts the use of the relationship based transient model of Menter et al. in blend with the Detached Eddy Simulation (DES) approach to two cases with huge level of flow division ordinarily considered hard to simulate. Firstly, the flow is solve on circular cylinder from  $Re = 10$  to  $1 \times 10^6$  giving drag crisis. The solution indicate great quantitative and subjective concurrence with the conduct seen in investigations. This case demonstrates that the methods works easily from the laminar cases at low  $Re$  to the turbulent cases at high  $Re$ . Besides, the flow is processed more than a thick air foil at high angle, for this situation the DU-96- W351 is considered. These reckonings demonstrate that a transient model is expected to acquire right drag forecasts at low angle, and that the blend of transient and the DES system enhance understanding in the profound slow down area.

**.Karim and Rahman (1996)** This paper presents limited volume system in view of Reynolds- found the middle value of Navier-Stokes (RANS) comparisons for calculation of 2D axisymmetric stream around uncovered submarine frame utilizing unstructured network. The body utilized for this intention is a standard DREA (Defense Research Establishment Atlantic) exposed submarine structure. Shear Stress Transport (SST)  $k-\omega$  model has been utilized to mimic turbulent stream past the structure surface. At last, figured results utilizing unstructured matrix are contrasted and those utilizing organized network furthermore with distributed exploratory estimations. The registered results demonstrate great concurrence with the test estimations.

### **2.3 VARIATION OF DRAG COEFFICIENT FOR DIFFERENT RANGE OF REYNOLDS NUMBER**

Many researcher has done good work and research to explain how the drag coefficient of the body varies with the change of Reynolds number. Some of the research predict the value of drag Coefficient for different range of Reynolds number for circular cylinder, wavy cylinder, square cylinder etc.

**Roshko (1961)** carried out the measurements on a large circular cylinder in a pressurized wind tunnel for Reynolds numbers ranges from  $10^6$  to  $10^7$  and showed that at high Reynolds number transition of drag coefficient increases from its low supercritical value to a value of 0.7 at  $Re =$

$3.5 \times 10^6$  and then the values are constant. The definite vortex shedding occurs, with Strouhal number 0.27 for the Reynolds number more than  $3.5 \times 10^6$ .

**Achenbach and Heinecke (1981)** they investigated vortex shedding phenomena and effect of relative roughness on drag for the flow past circular cylinder in the range of Reynolds number  $6 \times 10^3$  to  $5 \times 10^6$ .

**Shih and Wang et al (1993)** the effect of Reynolds number on the distribution of pressure is studied at low value of  $Re$ . The model of three different relative roughness for cylinder was tested on the low turbulence pressure tunnel. The test showed how the coefficient of pressure depends on  $Re$  and roughness, with the increase in roughness the pressure coefficient happens to be independent of  $Re$  when the  $Re$  is above  $2 \times 10^6$ .

**P Catalano, Wang and Parviz (2003)** The viability and accuracy of large-eddy simulation (LES) with wall modeling for high Reynolds number complex turbulent flows is investigated by considering the flow around a circular cylinder in the supercritical regime. A simple wall stress model is employed to provide approximate boundary conditions to the LES. The results are compared with those obtained from steady and unsteady Reynolds-averaged Navier–Stokes (RANS) solutions and the available experimental data. The LES solutions are shown to be considerably more accurate than the RANS results.

**K. Mahesh, and Moin (2003)** DNS was performed at cylinder Reynolds numbers of 20, 100 and 300, and LES was performed at a Reynolds number of 3900. The results obtained from the  $Re = 3900$  LES. Global variables such as recirculation length, separation point, and profiles of the mean velocities and turbulent Reynolds stresses are seen to be in good agreement with experiments.

**Lee and Cheol (2004)** flow control method has been investigated. The flow control method that had been proposed are: The first method that controlling the shear layers separation and the second method controlling surface flow over the bluff bodies. A small rod was setup on the upstream of the bodies to control the separation of shear layers, while to control the surface flow different Reynolds number ranges from  $1.5 \times 10^4$  to  $6.2 \times 10^4$  was set.

**Timmer and Schaffarczyk (2004)** The modified airfoil was studied and wind tunnel measurement was performed and found that the higher Reynolds numbers had a positive effect on the section roughness sensitivity, due to thinner and more stable boundary layers. The use of wrap-around Carborundum 60 roughness led to significantly more loss of maximum lift than

the use of zigzag tape, due to increased boundary layer thickness. The maximum lift/drag ratio decreased with increasing Reynolds number.

**Mittal and Singh (2005)** a numerical model solving the unsteady incompressible two dimensional Navier-Stokes equations was applied to studied the instability of shear layer and drag effect over the flow past a circular cylinder for Re ranges from  $10^0$  to  $10^7$ .

**Triyogi et al. (2009)** used of passive control method to reduce the drag over the I-type small cylinder was carried out, the cutting angle of  $\theta_s = 65^\circ$  is provided as passive control.

**M. Sami and M. Salih (2009)** The computational results for streamline patterns, vortices contours, velocity distributions, and drag and lift force coefficients are compared with those of the experiments to examine the effect of mesh size on the numerical simulations using the three turbulence models.

**Chang-yue et. al. (2010)** Numerical investigation of the compressible flow past a wavy cylinder was carried out by means of an LES technique for a free-stream. The mean drag coefficient of the wavy cylinder is less than that of a corresponding circular cylinder with a drag reduction up to 26%.

**Larose Guy and Steve (2012)** presented the investigation of reducing drag for a speed skater due to the turbulence effect of wind. The different range of Reynolds numbers are considered for calculating the drag coefficient. The flow separation over circular cylinder results in high dynamic drag force.

**Butt and Egbers (2013)** Flow over circular cylinders with the hexagonal patterned surfaces is investigated and discussed taking Reynolds numbers ranging from  $3.14E+04$  to  $2.77E+05$  into consideration and the well-known characteristics of flows over rough surface. The investigations revealed that a patterned cylinder with patterns pressed outwards (can be referred as hexagonal bumps) has a drag coefficient equal to 65% of the smooth one.

**M. Mallick and A. Kumar (2014)** a comparison has been made between the co-efficient of drag obtained by two methods. The co-efficient of drag obtained by weighing method is more accurate than those obtained from pressure distribution method. The drag force increases with increase in diameter of the cylinder. Also, for a cylinder of particular diameter, drag force has been found to increase with increase in air velocity.

## 2. 4 REDUCTION OF DRAG FOR A CIRCULAR CYLINDER

**Lemay and Bouak (2001)** the value obtained for the single cylinder is about 32% less than of the reduction of mean drag coefficient by claimed other authors. This result gained at  $Re$  values ranging from  $1.5 \times 10^4$  to  $4.0 \times 10^4$ ,  $S/d=2.55$ , and  $ds/d=1.25$ .

**Grosche and Meier (2001)** an experimental study has been carried on the bluff body and its aerodynamics. Paper includes the research for the drag reduction as follows: (a) providing passive ventilation on the wake region of the body in order to reduce the drag over the body, (b) optimization of shape can efficiently reduce the drag as well as trailing of vortices for the automobiles, (c) understanding the cause of loud noise and its source for the high speed trains, (d) the separation of flow are delayed on active flow control.

**Tsutsui and Igarashi (2002)** reduction of drag around the circular cylinder submerged in the air stream was investigated. It show that the pressure distribution around the small cylinder as symmetry all over the surface. The formation of quasi-static vortex among the I-type small and large cylinder, results in zero or negative value of pressure coefficient at the front portion of cylinders, while the pressure coefficient ( $C_p$ ) attains the maximum value of 0.1-0.2 at the region where the separated shear layer gets reattached. The different I-type small cylinders are used to reduce the drag over the large cylinder, implying passive control method. The I-type cylinders are formed by cutting them at certain angle ( $\Theta$ ) parallel to their axis. The different cutting angle are:  $\theta=0^\circ$  (circular),  $10^\circ$ ,  $20^\circ$ ,  $30^\circ$ ,  $45^\circ$ ,  $53^\circ$  and  $65^\circ$ . The Reynolds number was set as per the free flow velocity and the diameter of the cylinder i.e.  $Re=5.3 \times 10^4$ . The cutting angle  $\theta=65^\circ$  provide good results in the reduction of drag over the large circular cylinder placed at downstream as compared with the other cutting angles and gives 0.52 times less drag than that of a single cylinder.

**Alma and Moriya (2003)** the two cylinders are suited side-by-side for studying the characteristics of vortices, varying force of fluid, and wake formation behind the object. The different shape of cylinders are considered i.e. two circular cylinder as well as two square cylinder for the test. The vortex shedding in transitional flow was found to have a dominating character in both different shape of cylinders. For different gap spacing ( $T$ ) between cylinders of diameter ( $D$ ) considered as  $T=D>0:20$  in which lift force was found to be repulsive on both case, while in  $T=D\frac{1}{4}:10$ , the lift force acting on the cylinder results inward narrow wake and outward wake on the other cylinder.

**Pasto (2008)** the laminar and turbulent flows are considered to study the behavior of circular cylinder vibrating freely. The experimentation was done on the wind tunnel with varying roughness of cylinder and mass-damping. The vortex-induced vibration was noticed on the cylinder in the critical regime.

**Mohammad and Islam et al. (2010)** in the fluid mechanics and aerodynamics, drag force has important role to play for all type of object moving in the fluid. In some circumstance, drag can be undesirable for causing structural damage, consuming more power, decreasing speed for automobile, and high consumption of fuel. Therefore, it's important for the researcher to reduce drag by adapting or changing different parameter for different object. In this topic, a circular ring has been attached to the circular cylinder for reducing the drag. The drag force was obtained by external balance method, first drag for the cylinder without ring was recorded than with the ring attached to cylinder was calculated. The experimentation shows that the drag on the cylinder without ring was less than that of the cylinder with the ring this was because the ring increases the projected area of the plain cylinder and results in more attached flow. The maximum percent reduction of drag was found to be 25%, when ring was 1.3D and approximate value of aspect ratio was 12 for the cylinder.

**Tamayol (2013)** the arrays of cylinder placed in the micro channel was experimented to understand the pressure drop on these cylinders. The geometrical parameters like height and width of the channel, diameter, and spacing among the cylinders. The Deep Reacting Ion Etching (DRIE) technique was used to verify the model and the pressure drop was measured by applying nitrogen flow for the span of 0.1 to 35 sccm. The performed research suggest the minimum pressure drop for the higher micro-cylinder diameter.

**M. Mallick and A. Kumar (2014)** the study was carried out on the cylindrical bodies with varying cylinders diameters, surface roughness and air velocity. A comparison for the drag coefficient and pressure distribution between the smooth and rough surfaces of the cylinders are presented. In the smooth surface cylinder, the separation angles for different diameter of cylinder calculation are found to be around  $80^{\circ}$ ~ $90^{\circ}$  on either side of the cylinder from the upstream stagnation point.

## 2.5 PRE-RESEARCH AND EXPERIMENTATION DONE ON BLUFF BODIES AND THEIR DRAG COEFFICIENT

The study includes different types of cylindrical objects and various parameter with surface roughness. The review describes the effect and nature of drag force on the bluff bodies and suggests a suitable method to reduce its effect to achieve fine efficiency of the body moving in a fluid.

**Aldridge and Hunt (1978)** a porous nature of circular cylinder was considered and fitted among the hemisphere solid with such arrangement the drag force and drag coefficient was measured for the  $Re$  value varying from  $10^4$  to  $2.6 \times 10^5$  and five aspect ratio value from 7.92 to 2.67. The recorded data and the calculation described that the increasing aspect ratio, increases the drag coefficients. Flow passing the cylinders are visualized and weak vortex are seen behind the solids. Therefore, if we can decrease the aspect ratio of the bodies which will ultimately reduce the drag affecting the solid bodies.

**Protas (2002)** we invested in distinguishing the physical components that go with mean drag alterations in the barrel wake stream subject to turning control in this paper. We contemplated basic control laws where the snag turns pleasingly with frequencies differing from half to more than five regular frequencies. In our examination we mulled over the solution of the numerical re-enactments at  $Re=150$ . All the re-enactments and analysis were performed utilizing the vortex system. We affirm the concerning mean drag lessening at higher compelling frequencies. The principle result is that progressions of the mean drag are accomplished by altering the Reynolds stress and the related mean stream amendment. It is contended that mean drag diminishment is joined with control driving the mean stream toward the precarious the fundamental stream.

**Richter and Petr (2012)** for the particle study, different shape particles are considered such as spherical and non-spherical. The fluid and heat was supplied over the particle of non-spherical shape and the drag was noted. The approach in semi-exact models, distributed relationships for drag coefficient and nusselt number are enhanced and the exactness of terminations produced for drag coefficient and nusselt number is examined in an examination with distributed models.

### 2.5.1 Cylindrical Bodies

**Balachander and Mittal (1995)** depicted the impact of three dimensional on the drag and lift force of ostensibly two-dimensional cylinder which is helpful to portray the variety of numerical solutions between two dimensional and three dimensional examination.

**Laurent and Michel (2007)** to study the wake of cylinder, active control method was followed for the  $Re$  value of 100 so that the stream is in the laminar. The results of the examination indicate the reduction of mean total drag as the managing function of time, harmonic radial velocity of revolving cylinder.

**Z.C. Zheng et.al. (2008)** experimented frequency range or recurrence extents are to be considered for both close and far from the common recurrence of wake vortex shedding. Thusly, the impacts of recurrence lock-in, superposition and de augmentation on lift and drag are changed in light of the spectrum investigation on past time for drag and lift. A transverse oscillating or wavering cylinder in a constant flow or stream is displayed to explore frequency impacts of flow instigated wake on drag and lift forces of the cylinder. Most likely, demonstrated unsteady or fluctuating fluid are simulated utilizing an inundated boundary technique in a stable Cartesian cell to foresee the stream structure around the cylinder and visualize how the integration and coordination of surface pressure and shear circulations gives lift and drag on the wavering cylinder.

## 2.6 SURFACE ROUGHENING OF CYLINDRICAL BODIES

The common method used to diminish the drag over the bluff bodies like cylinder, sphere is applying surface irregularity or roughness. Many researcher has shown how the drag reduces for the sphere e.g. dimpled surface of gulf ball, fuzz on tennis ball etc. It delays the flow separation, narrowed the wake and consequently reduce the pressure drag for the roughened sphere surface.

**Merrick and Girma (1982)** a few troubles are experienced while analysing the super-critical regime with high Reynolds number for the stream over surfaces curvature of a building in a low velocity wind tunnel because of the sensitive to  $Re$ . Surface harshness on the exterior of the cylinder can influence the area of the detachment point and the degree of the wake on the rear face, whereupon the wind-incited reactions are subordinate. This study endeavours to control the stream around a ring-shaped cylinder through the use of counterfeit surface roughness over the outside of the cylinder. Later, the measure of the counterfeit roughness will be related with  $Re$  variance through a computational fluid flow wind stream analysis. These

relationships will help in selecting the suitable manufactured roughness that will bring the boundary layer transition at a position resembling to super-critical  $Re$  examined. Some roughness examples were tried over the cylinder, which were subjected to air flow with change in the turbulence magnitude. Estimations of pressure dispersion over the body exterior have been acquired for the  $Re$  limit of  $1 \times 10^4$  to  $2 \times 10^5$  in a BLWT. The outcomes are directly applied on the models in low speed BLWTs where super-critical stream flow attributes are foreseen. They portrayed the impact of surface irregularity for stream flow over a body at high Reynolds number utilizing wind tunnel.

**Harvey and Bearman (1993)** the pressure dispersion over the cylinder was modified by giving the irregularity or harshness around the surface of the body like providing dimpled exterior, roughening by sticking sand paper of different grade.

**Nicolas and Lyotard (2007)** utilizing a constant ultrasound method, estimating the speed of sphere made of steel falling freely through fluid. Then again, arbitrary surface irregularity and/or high fixation polymer arrangements decreases the drag bit by bit and prevent the drag crisis. We additionally show a subjective contention which ties the drag diminishment saw in low fixation polymer results to the Weissenberg number and ordinary stress distinction.

## 2.7 DISTRIBUTION OF PRESSURE

**Josue and Libii (2010)** Handy activities were prepared and examined in a subsonic wind tunnel to survey the pressure circulations around a round cylinder in the flow. They permitted understudies to gather their own information and utilization them to understand how the pressure over the cylinder surface varies with two unique parameter: the area of a given point along the outline of the mid-cross cylinder segment and the value of the Reynolds number of the stream. Plotted information delivered curves fundamentally the same to those in the literature writing. Detailing of investigated solution showed how viscous flow behaves in the upstream portion of body in contrast to its downstream portion. The impact of the Reynolds number on the capacity of the viscous flow to recoup pressure on the downstream was illustrated.

**Rasim and Hodzic (2011)** in fluid mechanics, flight science or aerodynamics studies relative movement of air around the body from hypothetical and exploratory aspect. These two methodologies won't give the same results if we utilize hypothetical laws taking into account perfect ideal procedure, on the grounds that exploratory examination is the presentation of real and genuine Process. Wind passage tunnel is an instrument that can be utilized for trial examination. Consequences of pressure circulation around the cylinder, profited by exploratory



examination in wind tunnel are introduced in this study. Produced experimented results are contrasted and hypothetical results, and on the premise of that information certain conclusions are made.

**Rakibul Islam (2013)** a numerical study was carried on the circular cylinder at rest applying Favre-averaged Navier-Stokes equation and finite volume method was followed to solve the desired problem at  $Re$  value of  $10^5$  for the flow motion. Numerical perceptions and simulated solution are checked with the test results and with experiment works of different analysts. Distinctive flow phenomena, for example, flow division, pressure dissemination over the solid, drag and so on are additionally learned at diverse boundary conditions. In the event of smooth solid, the division plots for experimentation figuring are discovered to be around  $80\sim 90^\circ$  in either side of the solid cylinder from the upstream stagnation point. The drag coefficients for smooth solid surface are 0.771 and 0.533 for experimentation count separately and consequent changes in drag because of induced surface irregularity are illustrated. The critical surface irregularity was discovered to be around 0.004 with drag coefficient of 0.43. They portrayed partition plot for flow over the cylinder at low Reynolds number. They examined the impacts of surface irregularity on pressure and dynamic forces on a roundabout cylinder for the Reynolds number scope of  $6 \times 10^4$  to  $1 \times 10^4$  in mesh produced flow turbulent streams. They acquired irregular cylinder by wrapping the exterior with business sandpapers to create isolated areas and pressure dissemination comparing to a higher proportionate Reynolds number on a smooth barrel. The Reynolds number in the flow is gained by expansion of wind passage blockage or turbulent intensity. The mean and varying pressure disseminations on barrels or cylinder of distinctive surface harshness in smooth and turbulent flow are plotted. They demonstrated that the varying pressure for the irregular barrels at distinctive Reynolds numbers are near to that smooth barrel at supercritical Reynolds number. Accordingly he gave the database to further research on irregular or rough cylinder for Reynolds number more than  $1 \times 10^6$ .

**Pilla and Kumar (2012)** low Reynolds number are considered for predicting the drag and its coefficient for the cylinder. Flow are considered as sub-critical, critical, and super-critical with the increasing value of Reynolds number, which mainly affects the drag force of the substance. The study involve the flow past circular cylinder for the high value of Reynolds number i.e.  $10^8$  for the current research work, through the experimentation drag has been predicted for the cylinder and a curve was plotted for the change in the coefficient of drag with Reynolds number. Pressure circulation describe the drag importance on the physic of the object.

# CHAPTER 3

## COMPUTATIONAL MODELLING

---

### 3.1. General

The Experimentation and Computer-aided engineering (CAE) are the important tools used for the analysis of the system. CFD is one of the CAE tools, designed for analysing the problem involved in the fluid motion, heat exchange etc. it provides good approximate result and has certain advantage over the experiment approach as mentioned in the chapter 1. The optimisation of models are easily done by the computer based software like Auto-Cad, Ansys Design Modular and Solid Works. The governing differential equation of flow are converted to transport equation for the numerical algorithm which is later followed by the software for simulation purpose.

### 3.2. GOVERNING EQUATION AND NUMERICAL MODELS FOR CFD

The Numerical methods are very handy in solving the complex problem associate with model geometry, experimental procedure, setups, and solving high order differential equation that govern the fluid flow. These equations are the mathematical representation of *conservation laws* of the nature or say physics. The physical law of conservation for the fluid dynamics mainly follows the certain quantities to be conserved i.e. Mass; Newton's second law and the First law of thermodynamics.

### 3.3. GOVERNING EQUATION

To analyse the flow problem, CFD apply the governing equation which is based on the continuity equation; momentum equation and the energy equation.

#### 3.3.1. Continuity equation

The continuity equation is the mass conservation and is expressed in Cartesian coordinate as

$$\frac{\partial \rho}{\partial t} + \frac{\partial(\rho u)}{\partial x} + \frac{\partial(\rho v)}{\partial y} + \frac{\partial(\rho w)}{\partial z} = 0 \quad \text{Eq. (3.1)}$$

Where the  $V$  velocity of fluid at any point, is describe as the velocity component ( $u, v, w$ ) along the direction ( $x, y, \text{ and } z$ ) with  $t$  time. This equation is re-written for the incompressible fluid as the density remain constant throughout the flow .i.e.

$$\frac{du}{dx} + \frac{dv}{dx} + \frac{dw}{dx} = 0 \quad \text{Eq. (3.2)}$$

The mass applied or given as input to the domain of control volume is equivalent to the mass at the exit of the same control volume.

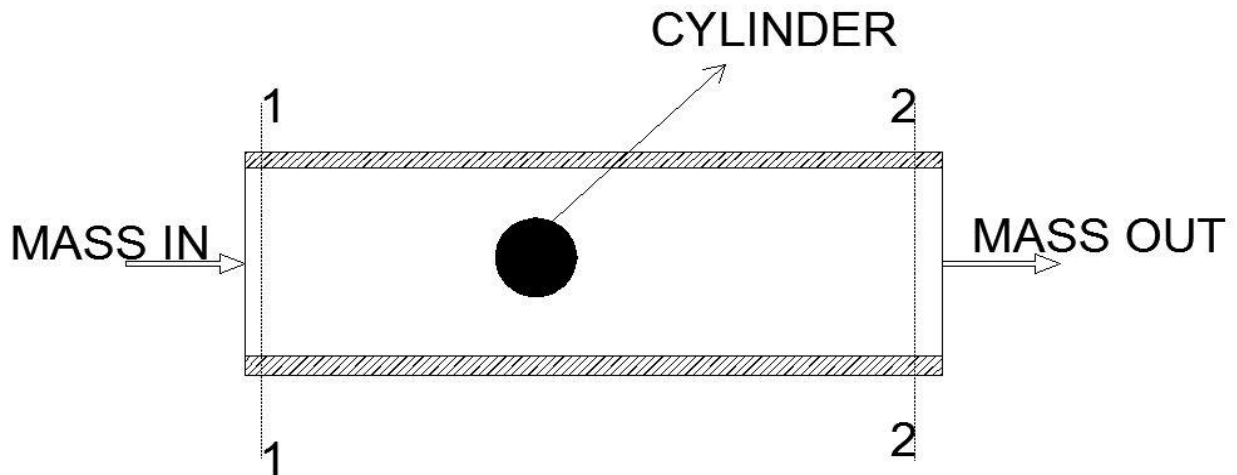


**Fig 3.1: Conservation of Mass in 2D domain**

The flow rate of mass for a given area of cross-section ( $A$ ), density of fluid ( $\rho$ ) and velocity of fluid ( $u$ ) is given as follows:

$$m = \rho Au \quad \text{Eq. (3.3)}$$

From the above figure it was clearly observed that the mass of fluid at inlet section 1-1 and mass escaping at outlet section 2-2 are conserved i.e. mass inlet,  $m_1$  is equivalent to mass outlet,  $m_2$ , which is mathematically represented as shown below:

$$m_1 = m_2$$

$$m_1 = \rho_1 u_1 A_1 \quad \text{And} \quad m_2 = \rho_2 u_2 A_2 \quad \text{Eq. (3.4)}$$

### 3.3.2. Momentum Equation

It is based on the second law of Newton, the forces acting on the particle of fluid element are equal to the product of element mass and its acceleration along the flow direction. In the flow, momentum conservation is also called as Navier-Stokes equation (Jiyaun tu, 2008) for 2D incompressible flow and neglecting body force is given as follows:

along x-direction

$$\frac{\partial u}{\partial t} + u \frac{\partial u}{\partial x} + v \frac{\partial u}{\partial y} = -\frac{1}{\rho} \frac{\partial p}{\partial x} + \nu \frac{\partial^2 u}{\partial x^2} + \nu \frac{\partial^2 u}{\partial y^2} \quad \text{Eq. (3.5)}$$

along y-direction

$$\frac{\partial v}{\partial t} + u \frac{\partial v}{\partial x} + v \frac{\partial v}{\partial y} = -\frac{1}{\rho} \frac{\partial p}{\partial y} + \nu \frac{\partial^2 v}{\partial x^2} + \nu \frac{\partial^2 v}{\partial y^2} \quad \text{Eq. (3.6)}$$

### 3.4. Design of Turbulence Models

Before carving the model for turbulent fluid flow, one must have a general idea of such flows and its characteristic. The nature of flow are describe by Reynolds number as mentioned in Chapter 1. If the  $Re$  value of the flow is above the critical Reynolds number  $Re_{cr}$ , the flow is termed as turbulent. The turbulent flow are characterized with random unsteady motion of the fluid stream and formation of wake in the object's rear. The property of flow like velocity etc. are seen to be fluctuating with time in the turbulent flow. The interaction of inertia and viscous phrase in the Navier-Stokes equation causes the flow to turbulent. The velocity  $v$  in the turbulent flow regime at an instantaneous time is composed of uniform mean velocity  $V$  and its fluctuating part  $v'(t)$ , which is superimposed to give  $v(t)=V+v'(t)$ . These fluctuating nature of turbulent flow have character of 3-D space and flow visualization method reveals the eddies with large range of turbulent scale.

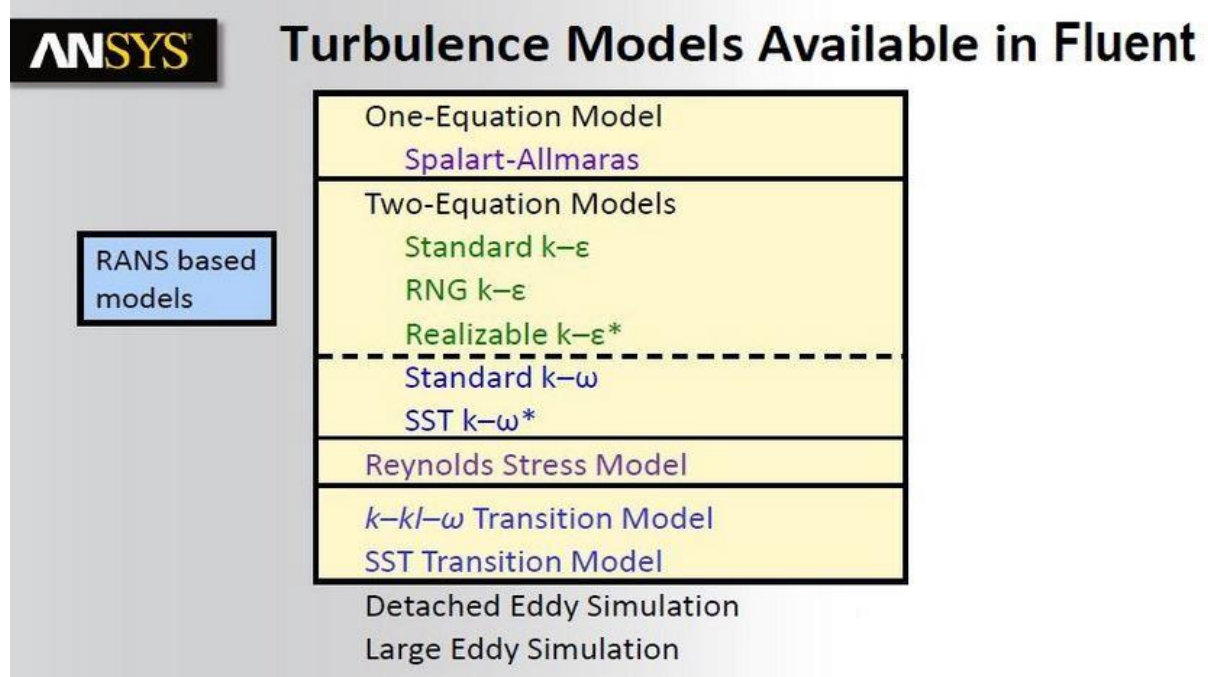
#### 3.4.1. List of models

In fluent the models has been classified as per the number of equation used and according to the nature of the fluid that need to be solve. The available models in ANSYS Fluent are listed below:

- Laminar viscous model
- Turbulence viscous model

The present study deal with the turbulence flow around the cylinder as the calculated Reynolds number is more than the critical Reynolds number. “The critical Reynolds No. ( $Re_{cr}$ ) for flow around the cylinder is given about  $Re_{cr}=2 \times 10^5$ .”(Cengel, 2014).

The involving turbulence model are shown in table1:



ANSYS		Turbulence Models Available in Fluent
RANS based models	One-Equation Model	Spalart-Allmaras
	Two-Equation Models	Standard k-ε RNG k-ε Realizable k-ε*
		Standard k-ω SST k-ω*
		Reynolds Stress Model
		k-kI-ω Transition Model SST Transition Model
		Detached Eddy Simulation
		Large Eddy Simulation

**Table 3.1: Turbulence Model**

In CFD, the time-dependent flow properties like mean velocity, mean pressure etc. are solve by the time-averaged equation or RANS equation given by ANSYS Tutorial as shown below:

### ANSYS RANS Modeling : Averaging

- After decomposing the velocity into mean and instantaneous parts and time-averaging, the instantaneous Navier-Stokes equations may be rewritten as the Reynolds-averaged Navier-Stokes (RANS) equations:

$$\rho \left( \frac{\partial \bar{u}_i}{\partial t} + \bar{u}_k \frac{\partial \bar{u}_i}{\partial x_k} \right) = -\frac{\partial \bar{p}}{\partial x_i} + \frac{\partial}{\partial x_j} \left( \mu \frac{\partial \bar{u}_i}{\partial x_j} \right) + \frac{\partial R_{ij}}{\partial x_j} \quad R_{ij} = -\rho \overline{u'_i u'_j} \quad \dots \text{Eq.(3.7)}$$

(Reynolds stress tensor)

- The Reynolds stresses are additional unknowns introduced by the averaging procedure, hence they must be modeled (related to the averaged flow quantities) in order to close the system of governing equations

→ 6 unknowns ...

$$R_{ij} = -\rho \overline{u'_i u'_j} =$$

$$\begin{pmatrix} -\rho \overline{u'^2} & -\rho \overline{u'v'} & -\rho \overline{u'w'} \\ -\rho \overline{u'v'} & -\rho \overline{v'^2} & -\rho \overline{v'w'} \\ -\rho \overline{u'w'} & -\rho \overline{v'w'} & -\rho \overline{w'^2} \end{pmatrix}$$

.....Eq.(3.8)

The Reynolds stresses are solved by the two model given as we proceed further.

- The Reynolds Stress tensor  $R_{ij} = -\rho \overline{u'_i u'_j}$  must be solved
- The RANS equations can be closed in two ways:

**Reynolds-Stress Models (RSM)**

- $R_{ij}$  is directly solved via transport equations (modeling is still required for many terms in the transport equations)

$$\frac{\partial}{\partial t} (\rho \overline{u'_i u'_j}) + \frac{\partial}{\partial x_k} (\rho \overline{u'_k u'_i u'_j}) = P_{ij} + F_{ij} + D_{ij}^T + \Phi_{ij} - \epsilon_{ij}$$

.....Eq.(3.9)

- RSM is advantageous in complex 3D turbulent flows with large streamline curvature and swirl, but the model is more complex, computationally intensive, more difficult to converge than eddy viscosity models

**Eddy Viscosity Models**

• Boussinesq hypothesis

→ Reynolds stresses are modeled using an eddy (or turbulent) viscosity,  $\mu_t$

$$R_{ij} = -\rho \overline{u'_i u'_j} = \mu_t \left( \frac{\partial \overline{u}_i}{\partial x_j} + \frac{\partial \overline{u}_j}{\partial x_i} \right) - \frac{2}{3} \mu_t \frac{\partial \overline{u}_k}{\partial x_k} \delta_{ij} - \frac{2}{3} \rho k \delta_{ij}$$

.....Eq.(3.10)

- The hypothesis is reasonable for simple turbulent shear flows: boundary layers, round jets, mixing layers, channel flows, etc.

The Standard k-ε model was developed by Launder and Spalding, 1974. The transport equation for Standard k-ε model is given as follows:

**ANSYS Standard k-ε Model Equations**

**k-transport equation**

$$\rho \frac{Dk}{Dt} = \frac{\partial}{\partial x_j} \left[ \left( \mu + \frac{\mu_t}{\sigma_k} \right) \frac{\partial k}{\partial x_j} \right] + \mu_t S^2 - \rho \epsilon; \quad S = \sqrt{2S_{ij}S_{ij}}$$

production      dissipation

**ε-transport equation**

$$\rho \frac{D\epsilon}{Dt} = \frac{\partial}{\partial x_j} \left[ \left( \mu + \frac{\mu_t}{\sigma_\epsilon} \right) \frac{\partial \epsilon}{\partial x_j} \right] + \frac{\epsilon}{k} (C_{1\epsilon} \mu_t S^2 - \rho C_{2\epsilon} \epsilon)$$

inverse time scale

**coefficients**

$\sigma_k, \sigma_\epsilon, C_{1\epsilon}, C_{2\epsilon}$  ← Empirical constants determined from benchmark experiments of simple flows using air and water.

**turbulent viscosity**  $\mu_t = \rho C_\mu \frac{k^2}{\epsilon}$  .....Eq.(3.13)

Where k and ε must be given at boundary condition, which can be done by the help of simple mathematical form given as:

$$k = \frac{2}{3} (U_{ref} T_i)^2 \tag{Eq. (3.14)}$$

$$\epsilon = C_\mu^{3/4} \frac{k^{3/2}}{l} \tag{Eq. (3.15)}$$

Where,  $l=0.07L$ , L is the characteristic length,  $T_i$  is turbulence intensity.

The constant present in the transport equation are given as:

$$C_\mu = 0.09; \sigma_k = 1; \sigma_\epsilon = 1.3; C_{1\epsilon} = 1.44; C_{2\epsilon} = 1.92$$

In fluent, normal turbulence intensity ranges from 1% to 5%. The default value for it is 5%.

### 3.5. Discretization Technique

There are various numerical methods to solve governing equation for the conservation of fluid. These are available in numerous out of which few are stated below:

1. Finite Different Method
2. Finite Volume Method
3. Finite Element Method

As per the thesis need only finite difference and finite volume has been describe in this paper.

#### 3.5.1. Finite Difference Method

The finite difference method solves the partial differential governing flow equation. The grid and nodes of the computational domain represents the fluid flow. The Taylor series expansion method is employed to get the partial differential form of governing equation at nodes of domain. The Taylor expansion results in finite solution which is converted to algebraic form that are applied to each node of the computational domain for the analysis of the flow.

The conversion of differential equation to algebraic equation is done by the following three method stated below:

- a) Forward Difference
- b) Backward Difference
- c) Central Difference

#### 3.5.2 Finite Volume Method

In this method, governing equation in integral form are being discretizes spatially directly. The domain representing the flow are divided into finite small volume with contiguous nodes connecting the grids to each other. The parameter are solve at the centre of the grid resulting the conserved equation expression by the help of interpolation and quadrature formula. It can adopt the grid of all kind i.e. structured or unstructured grid etc.

For example the generic fluid parameter  $\phi$  form, the surface area is perpendicular to the volume surface as shown in Fig: 3.2. The projected areas  $A_i^x$  and  $A_i^y$  along the x & y direction respectively. The 2-D, volume integral 1<sup>st</sup> order derivative of  $\phi$  is given by Gauss theorem along the x-direction as follows:

$$\left(\frac{\partial \phi}{\partial x}\right) = \frac{1}{\Delta V} \int_V \frac{\partial \phi}{\partial x} dV = \frac{1}{\Delta V} \int_A \phi dA^x \approx \frac{1}{\Delta V} \sum_{i=1}^N \phi_i A_i^x \quad \text{Eq. (3.16)}$$

Where  $\phi_i$  = variable at surface;

N=No. of bounding surfaces.

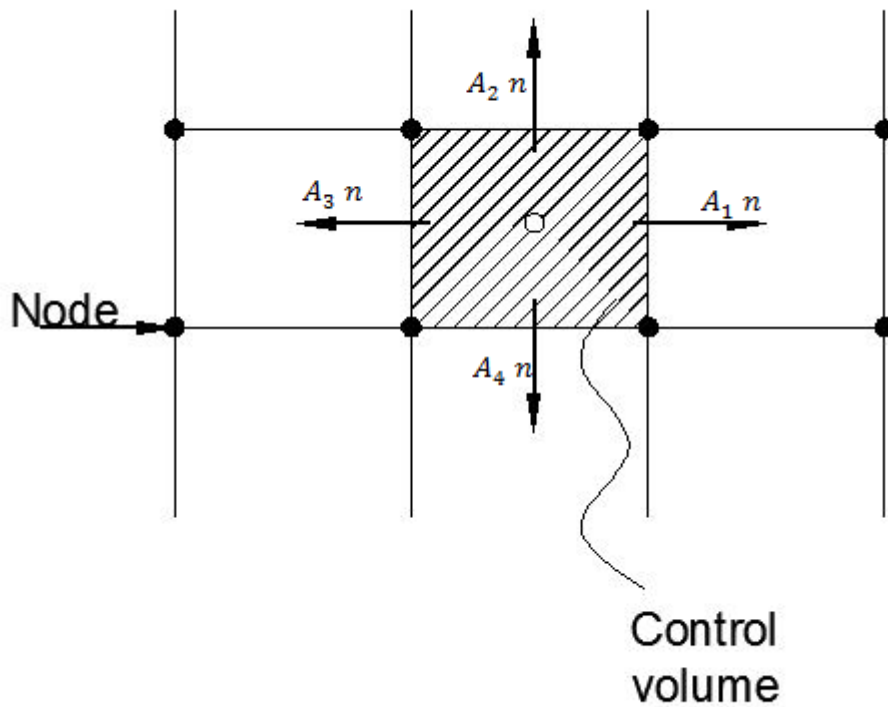


**Fig.3.2: Structured mesh for finite volume method**

### 3.5.3 Pressure-Velocity coupling

The flow chart has been shown, illustrating the working of SIMPLE SCHEME. The scheme uses the assumed pressure field for solving momentum equation and equation of pressure correction from the mass conservation is applied to have correct pressure field which is continuously improved by the interpolation till the solution is conserved.



# CHAPTER 4

## NUMERICAL ANALYSIS

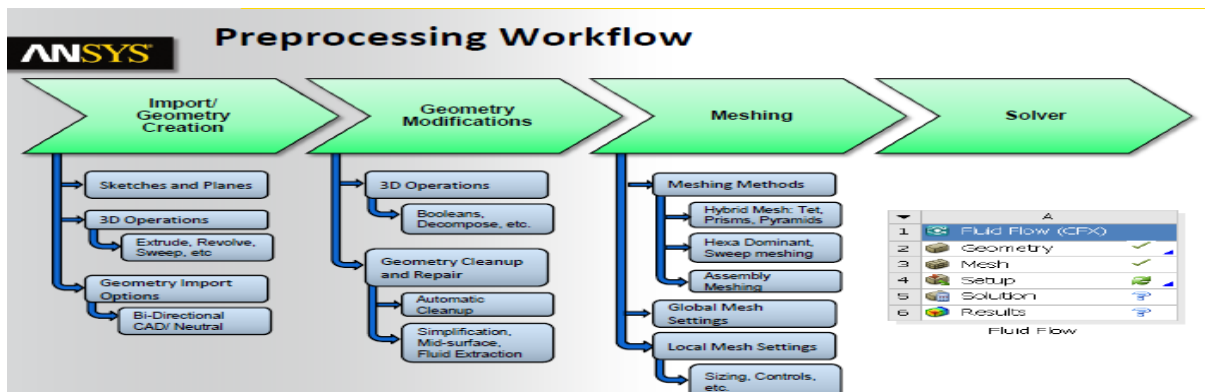
### 4.1.METHODOLOGY

The simulation procedure and steps followed were already been introduced in chapter 1. In this section we will stick to the rules of CFD solving technique and apply them to solve and to understand the flow around cylinder possessing rough surface. Before jumping into the solution we must be doctor to understand the nature of the problem that we are dealing with and then we look for the fittest method or model to eliminate the disease.

The current paper deals with the flow around the circular cylinder of different diameter, length and varying surface roughness. For the flow fluid air and water are taken into consideration of varying velocity to obtain the drag force imposed on the cylinder. To do this we follow the stepwise procedure starting with identification of objective or problem and going on to the proceeding steps as Pre-processing, solver which ends with Post-processing.

#### 4.1.1. PRE-PROCESSING

The process involves the generation or insertion of domain geometry used for calculation of force around the solids. All the modification like extruding the body, subtraction or addition process and generation of mesh are done over the domain.



Flow Chart.4.1 (Pre-process procedure)

#### 4.1.1.(a) Creation of Model and Domain

The geometry model and computational domain was prepared using the geometry tool called Design Modeller. This tools has quite important features including easy modification and simplification of shape, size and dimension of the geometry profile. It accepts the model geometry created using other software like CAD, Solid works etc. the parametric features of assigning the name to the geometry faces like inlet and outlet is possible. It involve two basic

operation of creating geometry i.e. 2D sketching and 3D modelling of solids. The experimental apparatus includes the rectangular chest with circular cylinder in it. The similar geometry model has been created in ANSYS Design Modeller and shown in figure (4.1)

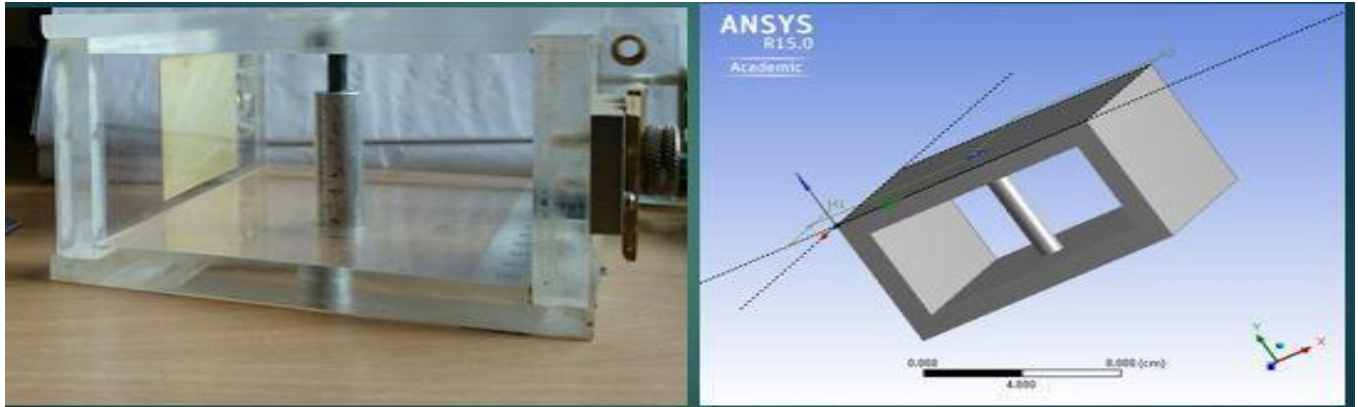


Fig 4.1 :( Replication of apparatus into ANSYS geometry model)

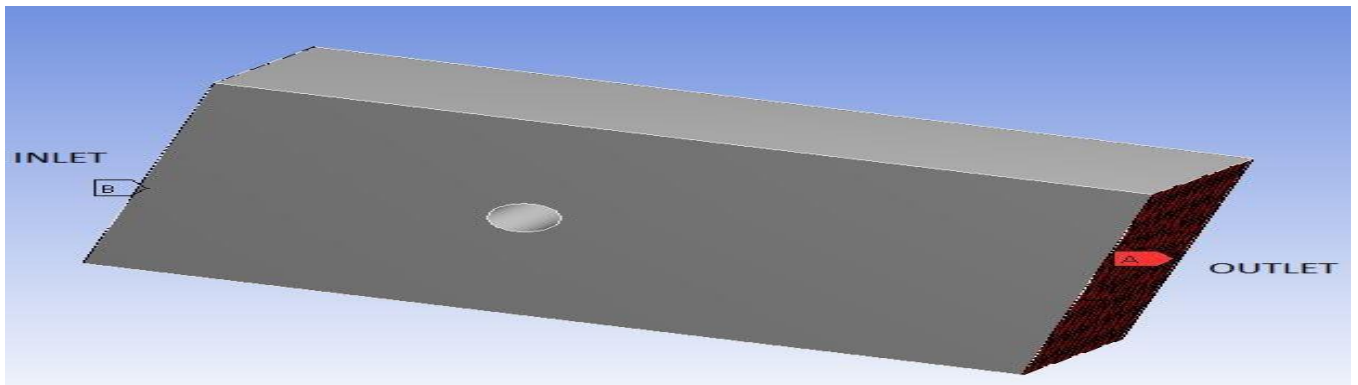


Fig4.2: (Computational Fluid domain)

The above figure (4.2) shows the computational fluid domain with inlet and outlet faces of the domain. The initial value at inlet are given in the solver part of the simulation process. The velocity parameter are given at this inlet face and pressure at outlet.

#### 4.1.1.(b) *Generation of Mesh for the Domain*

The computational domain is sub-divided into number of small element or cells called grid. There exists a two kind of grid formation known as structured and unstructured mesh. We apply the unstructured mesh for our solution domain in ANSYS Meshing as shown in figure (4.3)

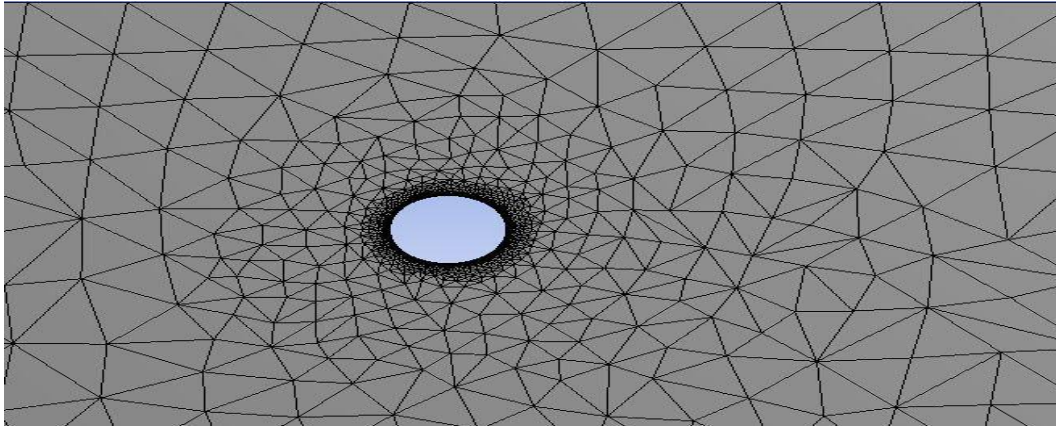


Fig4.3: Tetrahedral mesh of domain

The ANSYS meshing is adaptable in generating mesh for various physics obtain from CFD: PLOYFLOW, CFX and Fluent. The generated mesh helps in solving the governing equation flow at each cell or nodal points. The meshing technique is very important part of the numerical simulation process in order to capture boundary layer variation and to have easy convergence. The mesh discretized in these small cell to solve the Navier-Stokes equation. Therefore it is important to take special care about the mesh quality. The mesh quality are checked either by the orthogonal quality or by skewness of mesh. The range for the quality mesh is shown below:

Skewness mesh metrics spectrum					
Excellent	Very good	Good	Acceptable	Bad	Unacceptable
0-0.25	0.25-0.50	0.50-0.80	0.80-0.94	0.95-0.97	0.98-1.00

Orthogonal Quality mesh metrics spectrum					
Unacceptable	Bad	Acceptable	Good	Very good	Excellent
0-0.001	0.001-0.14	0.15-0.20	0.20-0.69	0.70-0.95	0.95-1.00

Table 4.1: Mesh quality

The quality of mesh for the prepared mesh for the domain are as follows:

**Mesh Quality:**

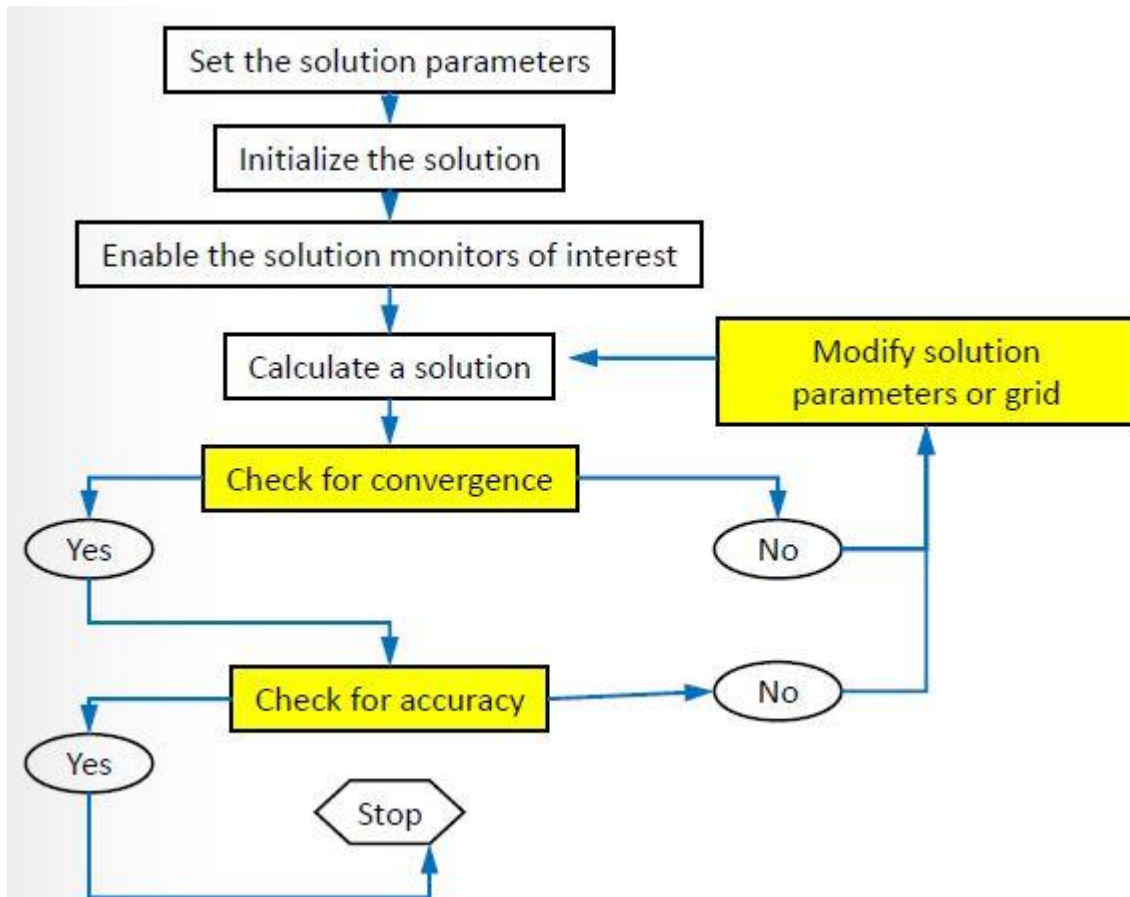
Orthogonal Quality ranges from 0 to 1, where values close to 0 correspond to low quality.  
 Minimum Orthogonal Quality = 7.17515e-01  
 Maximum Aspect Ratio = 7.10387e+00

Once we achieve the good quality mesh, can go for the solver portion for further analysis. If not, mesh are re-sized, re-fined or different type of mesh are given e.g. Hexa, prism, or multi-method mesh to have the desired quality of mesh. For discretizing the domain into mesh three well known method of Finite volume method, Finite difference method and Finite element

method are used. In this paper Finite volume method is employed to create unstructured mesh for the computational domain.

#### 4.1.2 Solver modelling for the Domain

In every analysis, there must be an input to have output as the result and this is done in the solver setting. The input parameters are initialized at inlet of the domain and necessary boundary condition are applied and calculation is carried out. There are few steps that need to be taken care of, such as selection of solver models and discretization schemes (i.e. finite volume, finite difference scheme). A flow chart is shown, describing the necessary steps to be carried out for the simulation. The analysis starts with setting of solution parameter i.e. Choosing solver and the solution are initialize to a point stating that the calculation from that point, we choose the inlet face as our point of initialization. Once the solution is initialized we can run the calculation.



Flow Chart 4.2: Steps for solver

Solver are of two types, Pressure based and Density based. We have used pressure based solver for our study as the flow is incompressible across the cylinder with Mach no less than 0.3. The

discretization scheme is done by selecting suitable Pressure-Velocity Coupling scheme in solution methods as shown below:

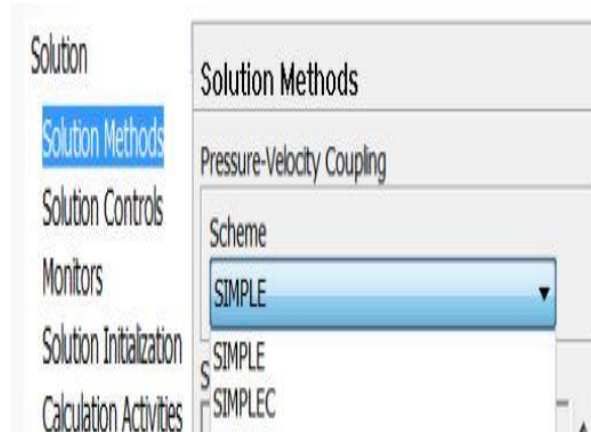
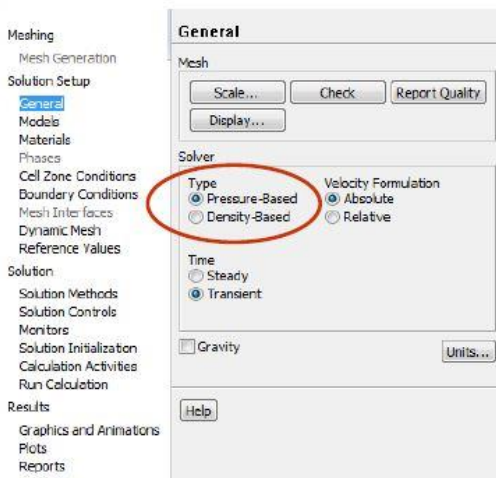


Fig. 4.4: Solver selection

Fig. 4.5: Choosing Pressure-Velocity Coupling scheme

After completion of running calculation the results are analysed and visualized in the next section of Post-processing.

### 4.1.3 Post-Processing

In Post-processing, the results obtained around the flow system are both quantitative and qualitative. It provides easy visualization of flow field through pressure, velocity contour and vector magnitude. Different types of plot like x-y; histogram etc. are easily obtain for the better analysis of simulated result. For the current study every contours, velocity profile and different plots are describe in the next chapter Discussion of Results.

The above mentioned methods and procedure are well followed to operate the simulation of flow around the circular cylinder.

## 4.2 PHYSICAL SETUP FOR THE STUDY AREA

For the simulation we need to create a computational domain of fluid with cylinder in it. The domain was prepared in Design Modeller in such a manner that the flow of fluid was along the x-direction and cylinder was placed perpendicular to the direction of flow field. According to the flow direction, the naming of the faces are done, which help in implementing the initial and boundary condition for the flow system. The well meshed domain is shown with the necessary boundary condition.

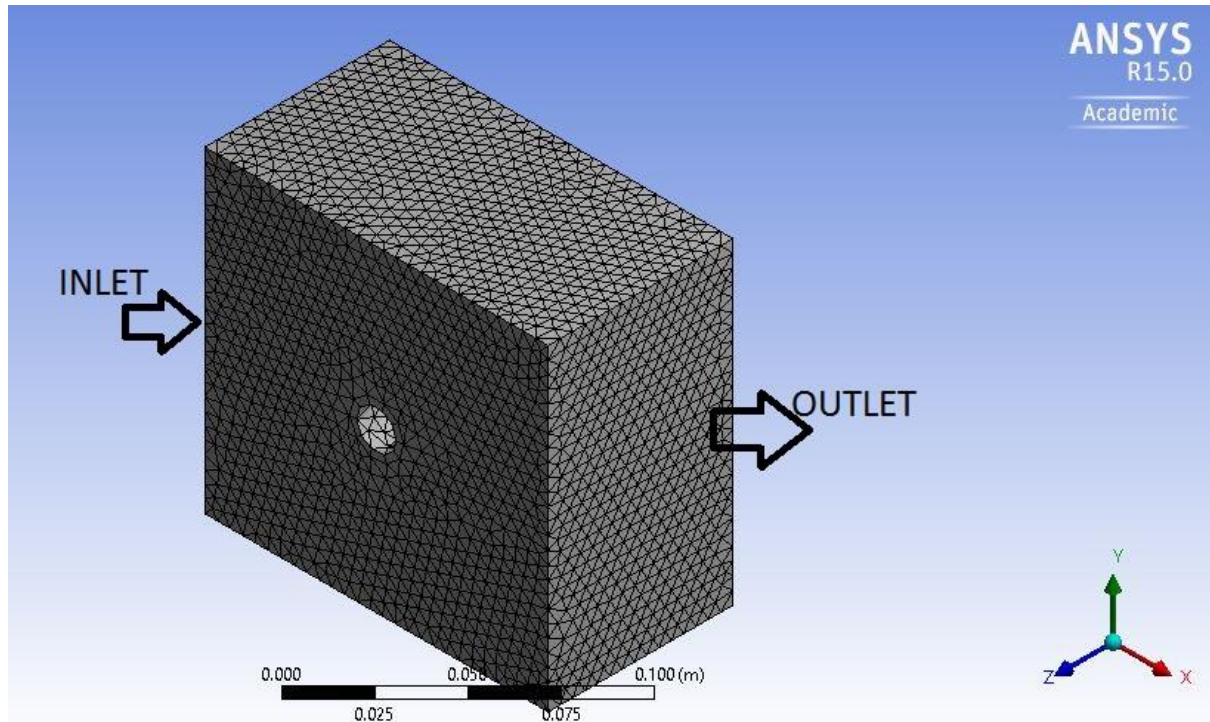


Fig 4.6: Flow field Domain

#### 4.2.1 Boundary and Cell Zone Condition

There are many different boundary condition that need to be applied to domain for doing the numerical simulation. The flow parameters are set at inlet, outlet, wall and the surface body. Boundary condition provided to the study area are as follows:

##### a) Inlet boundary condition

At inlet, the velocity of flow is considered and different velocities are given for different system. The range of velocity taken for the current study is from 8 m/s to 26.14 m/s so that the numerical results can be check with the experimental study. The velocity  $u_x$  imposed at inflow is along the x-axis so the velocity component (u, v, w) along (x, y, z) receptively is given as  $u=u_x$ ;  $v=w=0$  at the inlet. More details are provided in the chapter 5.

##### b) Outlet boundary condition

The outflow was set as pressure outlet, to have constant pressure outflow. For the present case the pressure taken is zero Pascal so that it will have low influence in the upstream inflow.

##### c) Wall and surface body condition

The wall is considered to be a stationary wall for both cylinder wall and rectangular box wall (i.e. conduit in which fluid flows) and no-slip condition is applied at these wall. The surface of the cylinder is provided with different roughness height ( $k_s$ ). The given surface height are in micron ranging as (82; 265; 348).

### *Cell Zone condition*

The small discrete cell are assigned material properties like fluid or solid as per the requirement. I have considered cell zone as fluid (i.e. air and liquid water) for solution of fluid problem. One could choose different material from the material database present in the Fluent.

## **4.3. Turbulence solution**

As described in chapter 4, the turbulence model say RANS model is used to solve the flow turbulence. We apply the Standard k- $\epsilon$  RANS model for the study flow past circular cylinder. The momentum equation and transport equation is employed for the numerical analysis given in chapter 3. The Fluent converts these equation into algebraic form using Finite volume method. The SIMPLE pressure correction technique is used. The solution was run and the drag force recorded as per the procedure.

### ***4.3.1 Wall Modelling***

The wall needs to be designed in such a manner that it captures all possible value required for the simulation. To use the wall function one must locate the 1<sup>st</sup> cell i.e.  $y^+$ , for low Reynolds No.  $y^+$  must not be less than 30.

# CHAPTER 5

## EXPERIMENTATION

---

### 5.1 General

In this chapter we are going to carry out few procedure that will determine the drag over the cylinder. When the air flows over the body it imposed normal thrust on the surface and parallel shear along the body surface. The application of pressure distribution method is described and used to measure the drag force over the cylinder of varying diameter, surface roughness at different air velocity.

### 5.2 Equipment used

The study involve the use of many apparatus starting from Air Flow bench to cylinders.. The pressure variance is observed through Multi-tube manometer. There are four circular cylinder of same length (70cm) with different radius i.e. (12.5, 10, 7.5, 6.25) mm are considered for the study of drag force and its coefficient variation varying air flow velocity. The different roughness parameter are taken to study the surface roughness effect on the drag force. The detail specification of cylinders dimension and roughness height are presented in table and theirs figures are shown:



**Fig.5.1: Smooth Surface Cylinders**

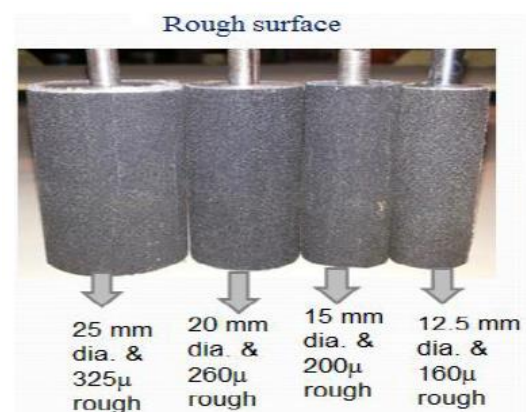


**Fig.5.2: Cylinders of Varying Roughness**



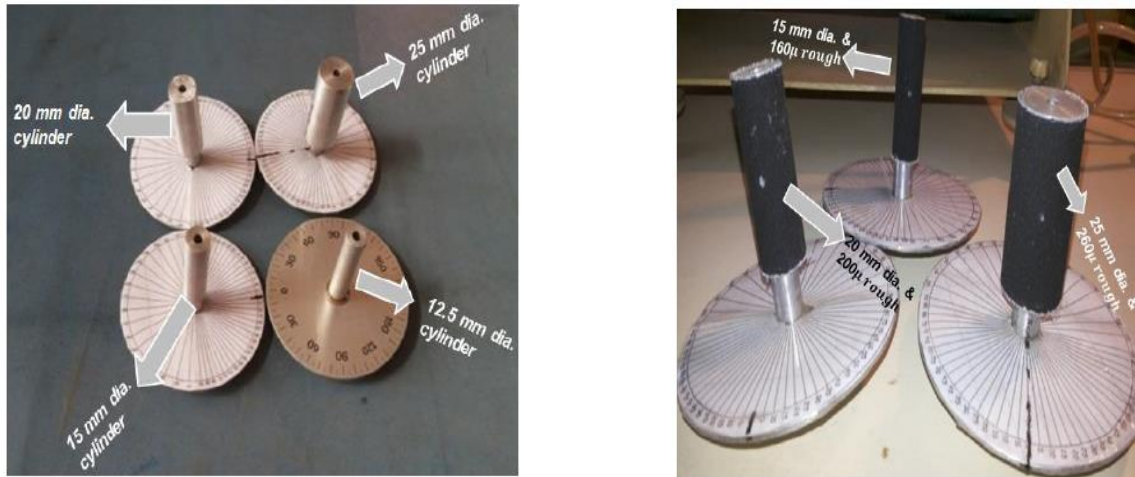


**Fig.5.3: Cylinders are fitted to circular disc having measuring angles imprinted on it.**

Table 5.1: Details of Geometrical parameters

Sl. No	Name of Apparatus	Description of Apparatus
1	Cylinder	Radius: (12.5, 10, 7.5, 6.25)mm; Length: 70mm
2	Air density	1.24 kg/m <sup>3</sup>
3	Barometric pressure	1.03 × 10 <sup>5</sup> N/m <sup>2</sup>
4	Gas constant	287.2
5	dynamic viscosity	1.983×10 <sup>-5</sup> kg/m-s
6	Roughness	(82,165,265,348)µm

### 5.3 Experiment Method and Procedure

The schematic picture of airflow bench is shown to describe the flow from air box through the test piece and various measuring points of temperature and multi manometer tube to measure the total and surface pressure over the cylinder. The flow velocity is control by the regulator which has quite value of range that specify the rate of flow. We use the dynamic pressure to calculate the free stream velocity V which is given as:

$$V = \sqrt{\frac{2(P_1 - P_2)}{\rho}} \quad \text{Eq. (5.1)}$$

Where P<sub>1</sub> = stagnation pressure;

P<sub>2</sub> = static pressure; and

ρ = density of fluid.

The value of  $P_1$  &  $P_2$  are obtained from Pitot-static probe used in the experiment.

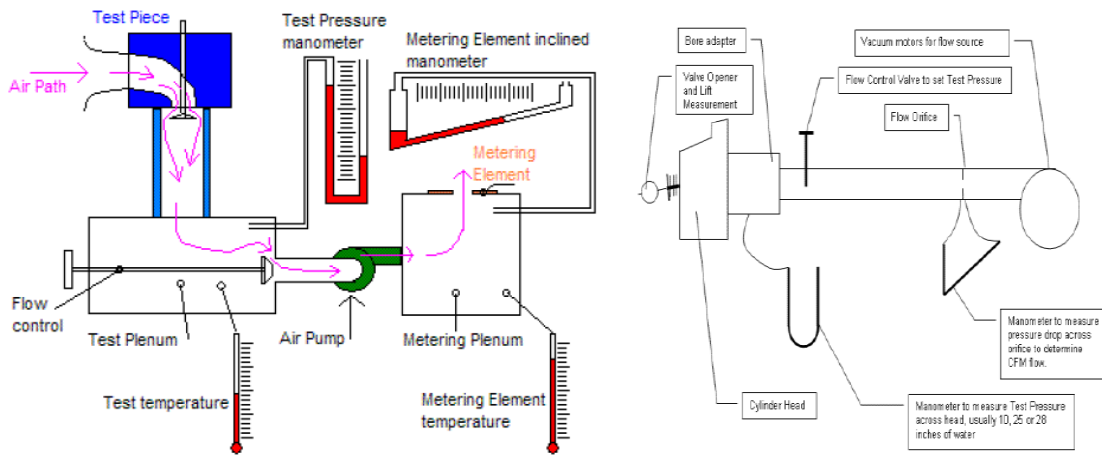


**Fig.5.4: Schematic picture of Airflow bench.**

### 5.3.1 Pressure Distribution Technique

To carry out the process we follow the certain steps of measuring the difference in pressure distribution over the circular cylinder which is the test specimen of the study. The procedure are listed below one after the other and the setup is shown for pressure measurement.



**Fig.5.5: Pressure Measurement Setup**

**Step1:** First the cylinders are joined to the calibrated disc showing division of angle in it. The cylinder is set at a zero angle and then the velocity regulator is set to maximum value. The initial barometric pressure and temperature are recorded. The manometer tube is connected to the cylinder for measuring the surface pressure. For measurement of total pressure and static pressure Pitot-tube is used. The total pressure obtain is rechecked with the box pressure which must be equivalent.

## EXPERIMENTATION

**Step2:** Once the all required instrument are fitted, the motor is on and the air flow starts. Now we record the total pressure, surface pressure and the static pressure from the multi-manometer tube for each  $5^{\circ}$  angle of rotation up to  $90^{\circ}$  and then from  $90^{\circ}$  - $180^{\circ}$  the cylinder is rotated at  $10^{\circ}$ .

**Step 3:** The above steps are repeated for different range of velocity and varying surface roughness.

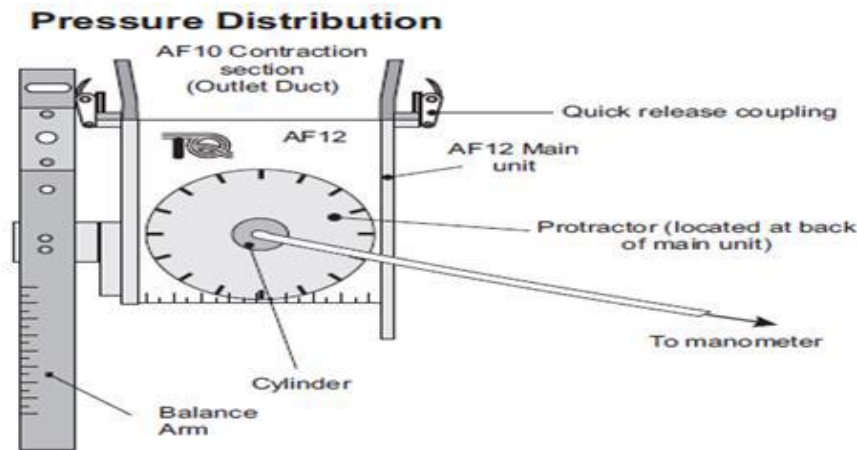


**Fig.5.6: Pressure Distribution Method**

When all the required data are obtained, calculate the drag coefficient by the help of the following equation:

$$C_D = \frac{1}{d} \oint (c_p \cos \theta + c_f \sin \theta) ds \quad \text{Eq. (5.2)}$$

Where,  $C_P$  is the pressure coefficient and given by:

$$C_P = \frac{P - p_0}{\frac{1}{2} \rho U^2} \quad \text{Eq. (5.3)}$$

Here,  $P$ = surface pressure;

$p_0$  = static pressure;

$\rho$  = air density;

$U$ = velocity.

The shear is neglected because the pressure force was found to be dominated, so only the term is considered for the calculation of drag coefficient. Therefore the Eq. (5.2) changes and is given as:

$$C_D = \oint_0^{2\pi} c_p \cos \theta d\theta \quad \text{Eq. (5.4)}$$

# CHAPTER 6

## DISCUSSION OF RESULTS

### 6.1 General

The investigation are carried out both numerically and experimentally and their results are obtained which will be detailed briefly in this chapter. The results shows the variation of drag force over the cylinder submerged in the flowing air and water under the influence of varying size of the cylinder itself, different surface roughness applied over the cylinder and by the change in the flow velocity. The drag force calculated by the method mentioned in chapter 4 & 5 are used and shown by the help of graph for different parameters.

### 6.2 Numerical Results

The drag force is calculated using ANSYS FLUENT for varying fluid velocity and various geometric parameter of the cylinder. In this section, the solution for drag will be subdivided according to the alteration of parameter that bring change in the total drag force.

#### 6.2.1 Flow velocity

The drag force is encountered for the varying flow velocity over the cylinder of constant diameter i.e. constant area. The graph is plotted in between the drag and the velocity for analysing the change in drag on cylinder with respect to the change in velocity.

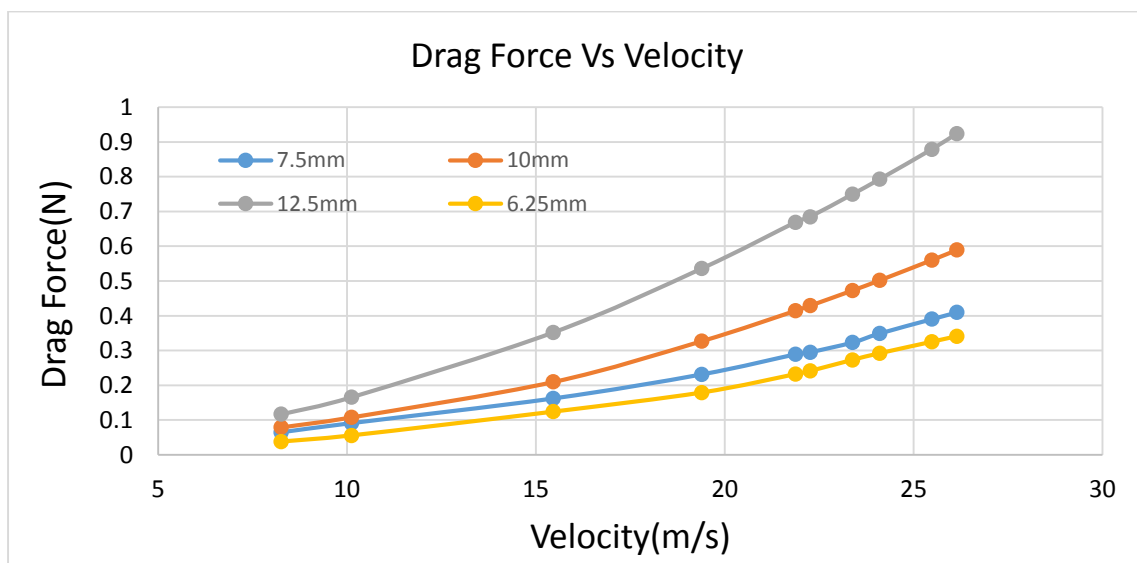


**Fig.6.1: Drag force on cylinder of radius (6.25, 7.5, 10, 12.5) mm**

## DISCUSSION OF RESULTS

There is increase in the drag force has been noticed for the increase in the flow velocity. It is because the drag is directly proportional to the velocity, so for the particular radius of cylinder drag force gets raise for the growing speed of the stream. Form the graph it is observed that at the low velocity nearly 8m/s there slight change in the drag which is due to laminar sub-layer.

### 6.2.2 Size of the cylinder

For this, velocity is kept constant and the size of the cylinder is being changed by increasing the radius of the cylinder. The graph of different uniform velocity for different radius is drawn. The effect of change in the radius change the projected area which is directly responsible for the drag force.

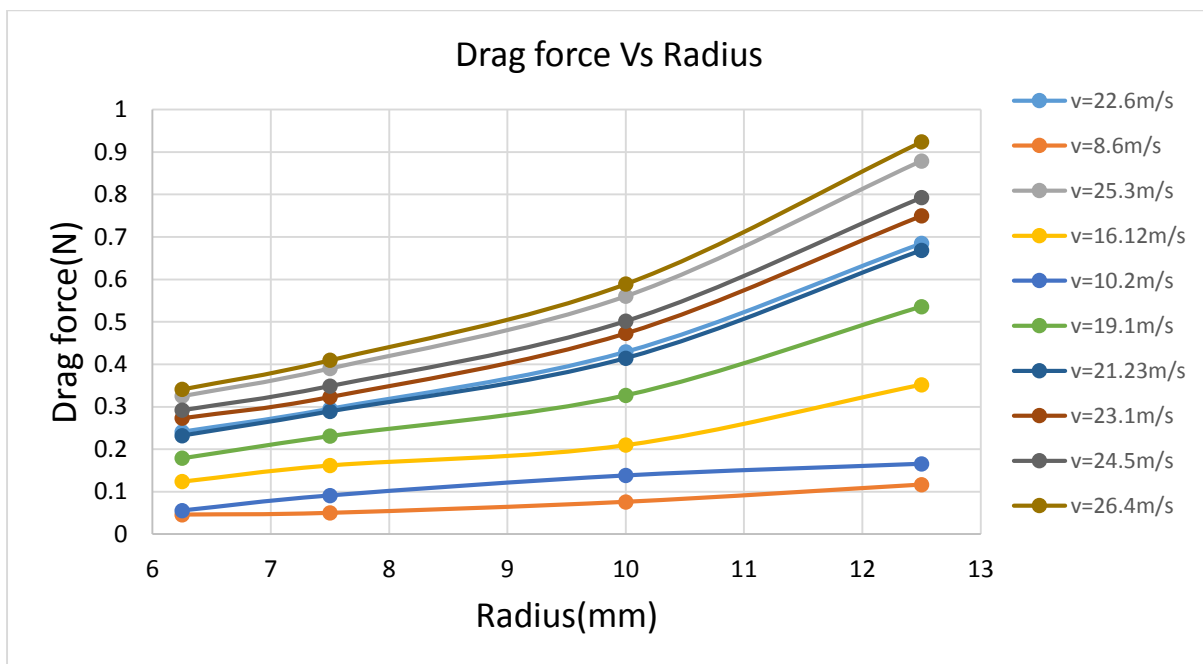


**Fig.6.2: Variation of Drag Force Due To Change in Area of the Cylinder**

The drag was found to be going up with the increase in the radius of the circular cylinder. The drag force is directly proportional to the area, thus when the radius of cylinder is increased the area of the cylinder gets bigger and consequently increases the drag force.

The length of the cylinder also plays the same role of increasing the drag when projected area of the cylinder gets increased due to increase in the cylinder length. This variation can also be observed by the plot shown:

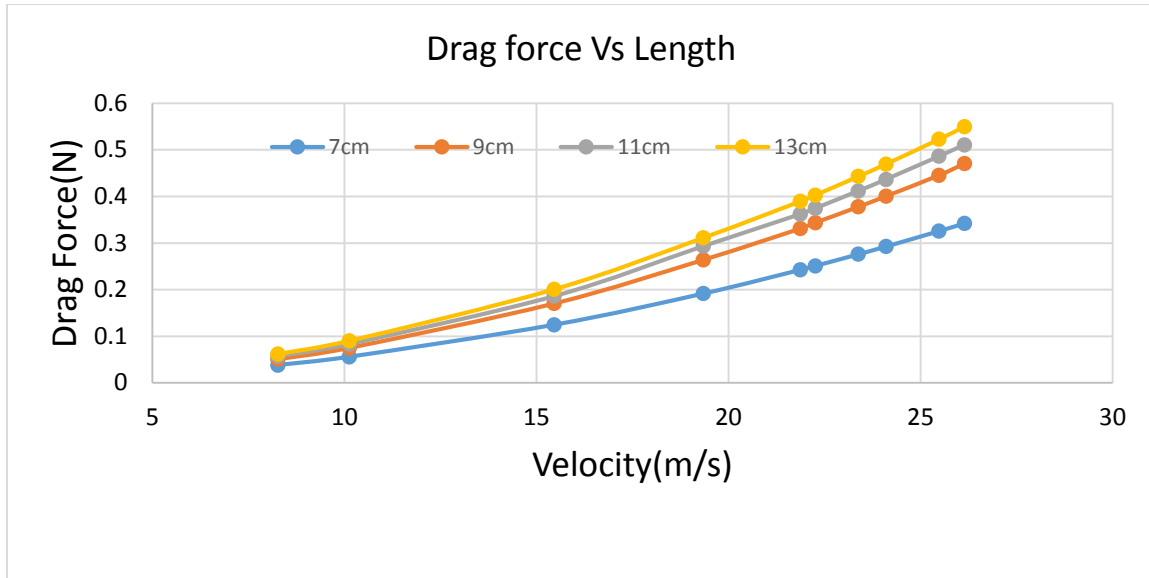


**Fig. 6.3: Variation of Drag Force with Varying Length of the Cylinder**

The different length considered for the calculation of drag are (7, 9, 11, 13) cm. the length variation for the evaluation of drag is only done in ANSYS as the experimental test box was of fixed length. One could run this experiment if condition allows, for the better understanding of drag variation with varying length of cylinder.

### 6.2.3 Surface Roughness

To check the effect of roughness in the drag force over the cylinder surface, the sand paper of different grade has been used and mentioned in table 5.1. The air is passed over the cylinder and the drag force report is noted down.

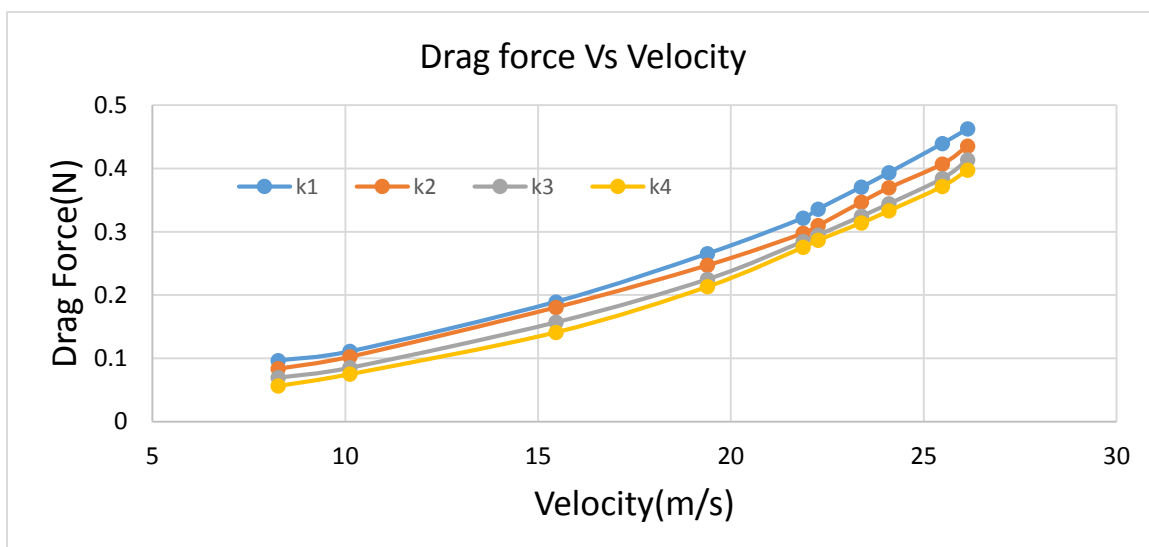


**Fig. 6.4: Different Roughness with varying Velocity.**

### DISCUSSION OF RESULTS

For the constant roughness, constant radius of 7.5 mm and varying stream velocity, the drag is increasing but it reduces the drag that obtained from the smooth cylinder.

The drag force for varying surface roughness at a constant velocity and constant radius of the cylinder is plotted and compared with the experiment data results for each radius.

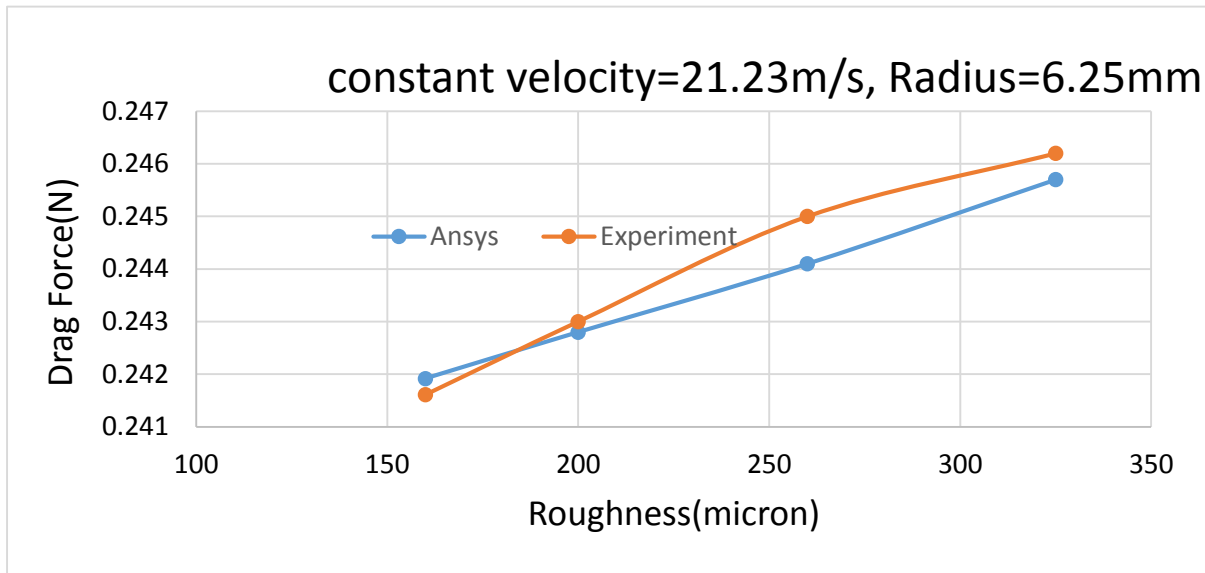


**Fig.6.5 Effect of roughness for R=6.25mm**

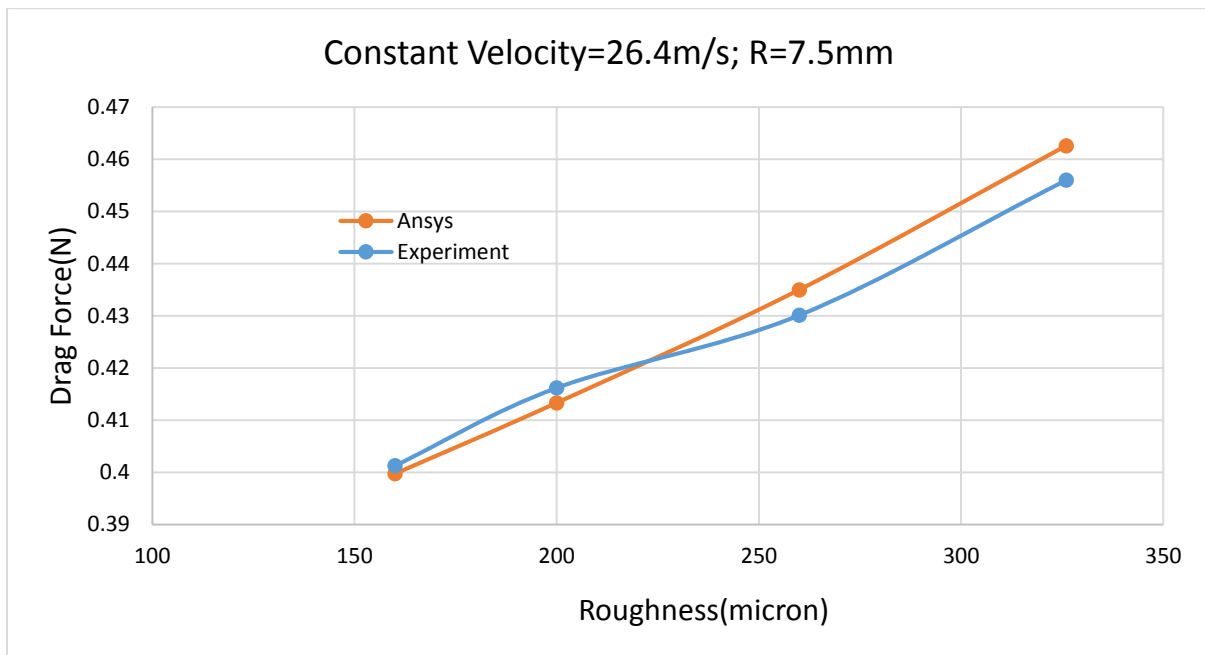


**Fig.6.6 Effect of roughness for R=7.5mm**

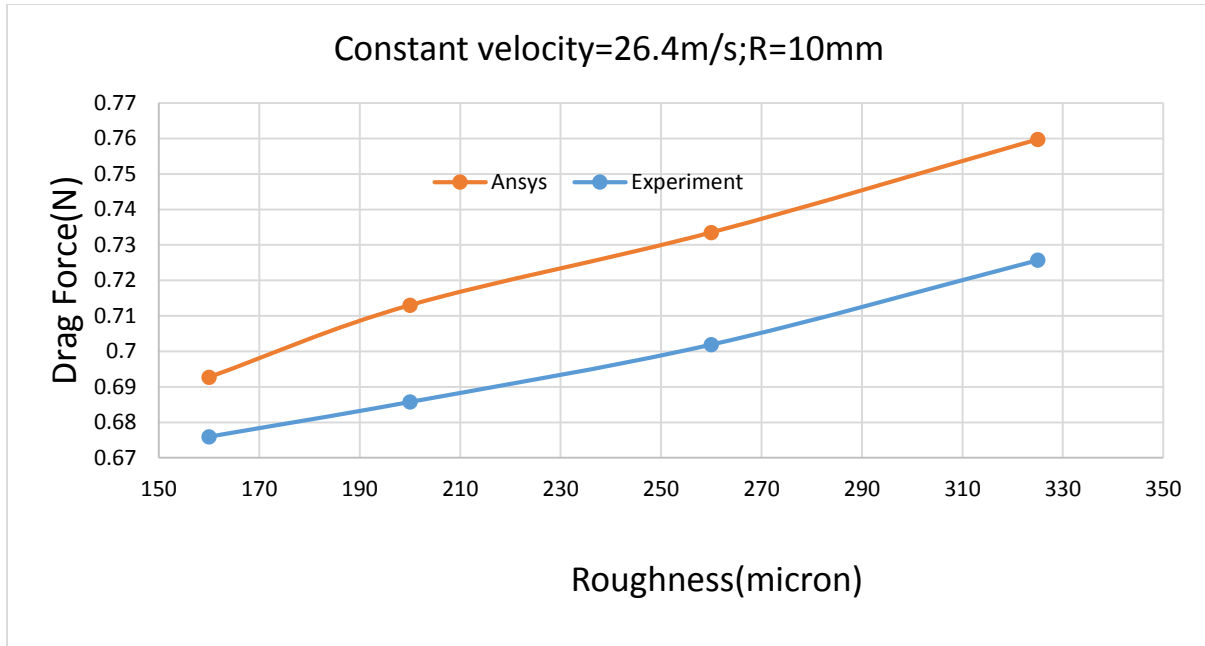


**Fig.6.7 Effect of roughness for R=10mm**

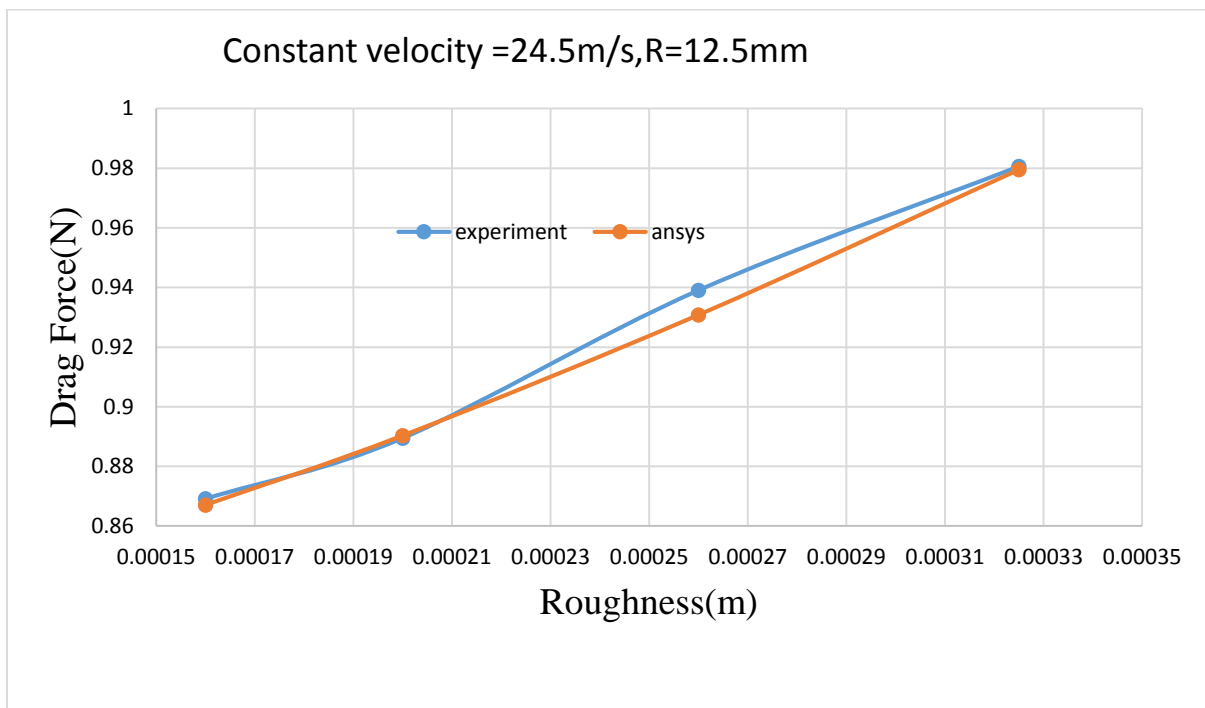


**Fig.6.8 Effect of roughness for R=12.5mm**

The drag calculated by the numerical and experiment study gives the relative results for varying roughness. As per the theory drag get reduces when the surface roughness is provided over the blunt bodies like cylinder and sphere, but the plot speaks differently, it shows the linear increment of drag violating the theory. There for further study is carried out with varying Reynolds No.



### 6.2.4 Reynolds Number and water as the fluid

The flowing fluid has been changed from air to water liquid in the ANSYS and simulation was processed for calculating the drag force over the cylinder. On modifying the fluid the fluid properties like density ( $\rho$ ) and dynamic viscosity ( $\mu$ ) also gets modified. Thus the value are given as:  $\rho = 1000 \text{ kg/m}^3$  &  $\mu = 8.90 \times 10^{-4}$ .

The graphs are been plotted for the range of Reynolds No. and particular cylinder having same radii.

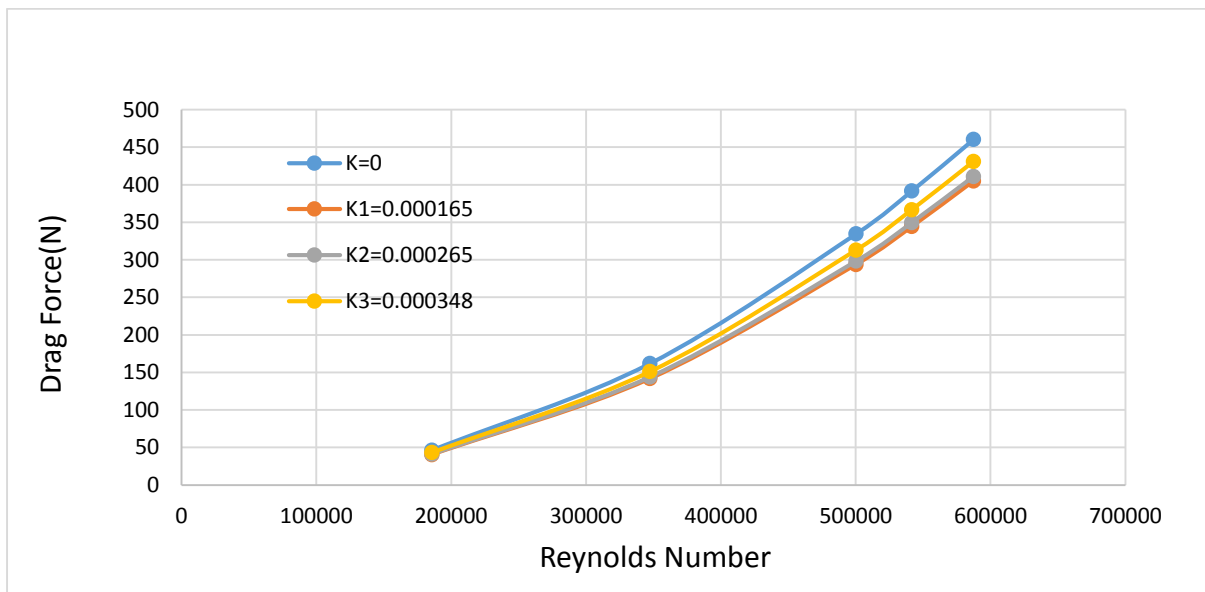


**Fig.6.9: Drag Vs Reynolds No. for R=10mm**

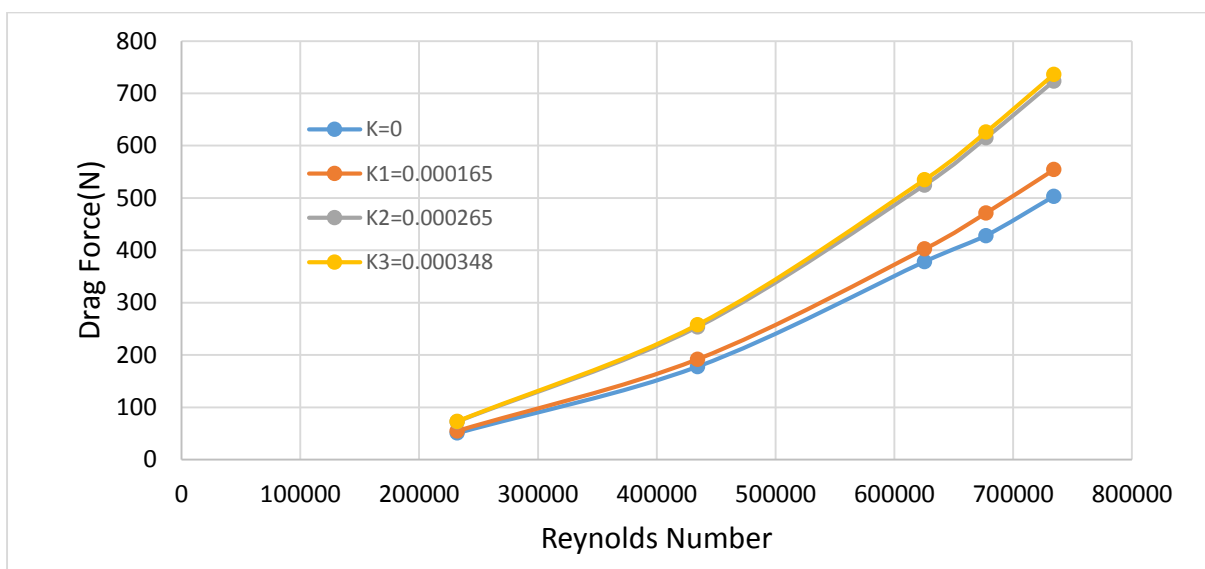


**Fig.6.10: Drag Vs Reynolds No. for R=12.5mm**

From the graph, it found to be believed that there is very slight change in the drag corresponding to the close value of roughness. The variation of drag coefficient can enlighten the drag dependence on the  $R_e$  value, which is displayed on the below plot.

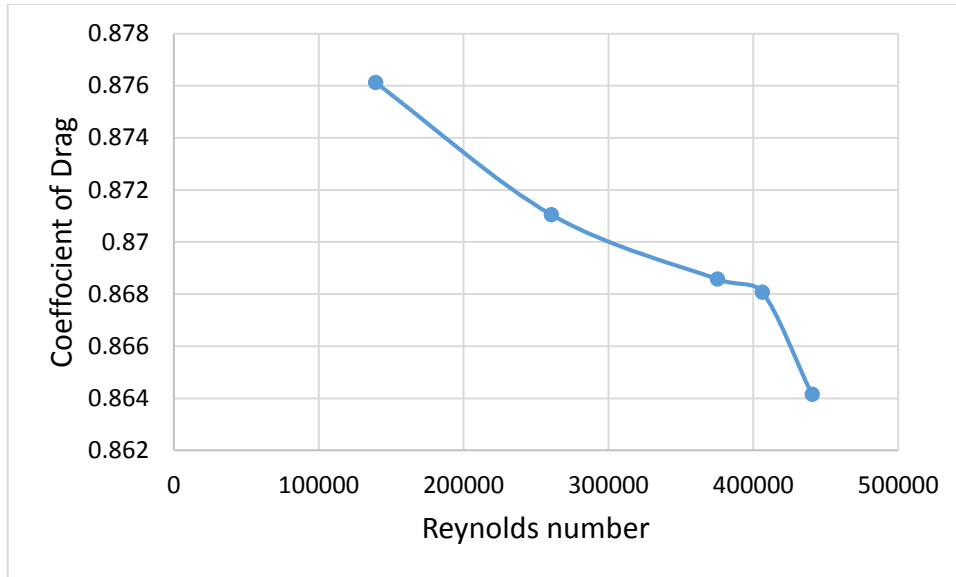


**Fig.6.11: Coefficient of Drag  $V_s$  Reynolds No. for  $R=7.5\text{mm}$ ;  $k_s=0\mu\text{m}$ .**

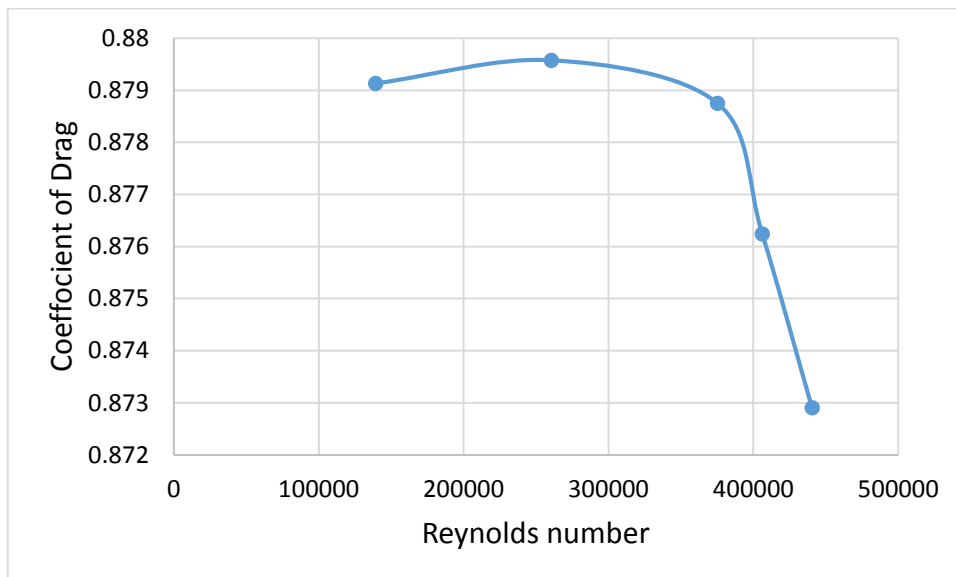


**Fig.6.12: Coefficient of Drag  $V_s$  Reynolds No. for  $R=7.5\text{mm}$ ;  $k_s=348\mu\text{m}$ .**

The fig.6.11 describe the reduction in the drag coefficient with increase in the Reynolds No. the flow is turbulent as critical value  $2 \times 10^5$  is exceeded for the flow. There linear decrease in the value of  $C_D$  as the surface of the cylinder is smooth and velocity is directly responsible for the cause. When the surface roughness is applied over the cylinder surface, the

*DISCUSSION OF RESULTS*

drag coefficient goes slightly up near the critical  $R_e$  value, then it get reduce after the approx. value of  $R_e = 3 \times 10^5$  as observed in fig.6.12.

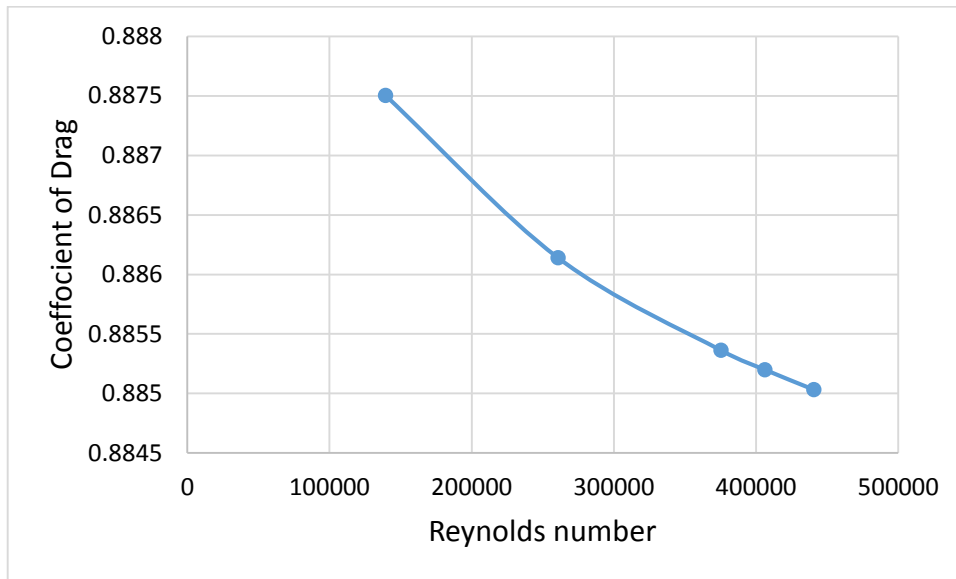


**Fig.6.13: Coefficient of Drag  $V_s$  Reynolds No. for  $R=7.5\text{mm}$ ;  $k_s=265\mu\text{m}$ .**

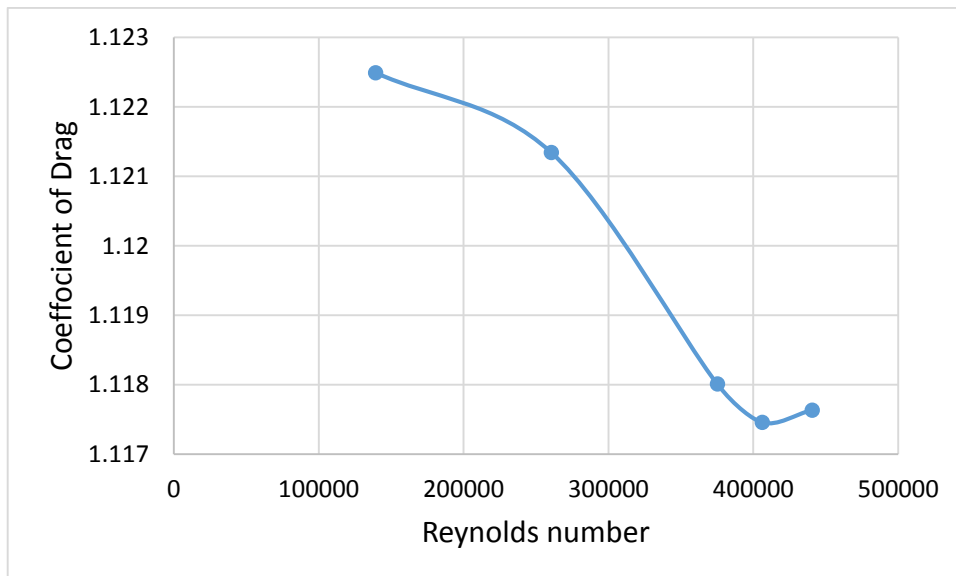


**Fig.6.14: Coefficient of Drag  $V_s$  Reynolds No. for  $R=7.5\text{mm}$ ;  $k_s=165\mu\text{m}$ .**

The repetition of providing roughness gives the reduced drag as compared to the smoother one, but not much difference is seen over the variation of  $C_D$ .

### 6.2.5 Contour

The different contour like pressure contour and velocity contour are shown to study the pressure and velocity distribution over the cylinder. The velocity vector magnitude is also obtained and presented.

a) *Pressure contour:*

The pressure contour for different radius of cylinder is presented with the constant velocity of 22.6 m/s.

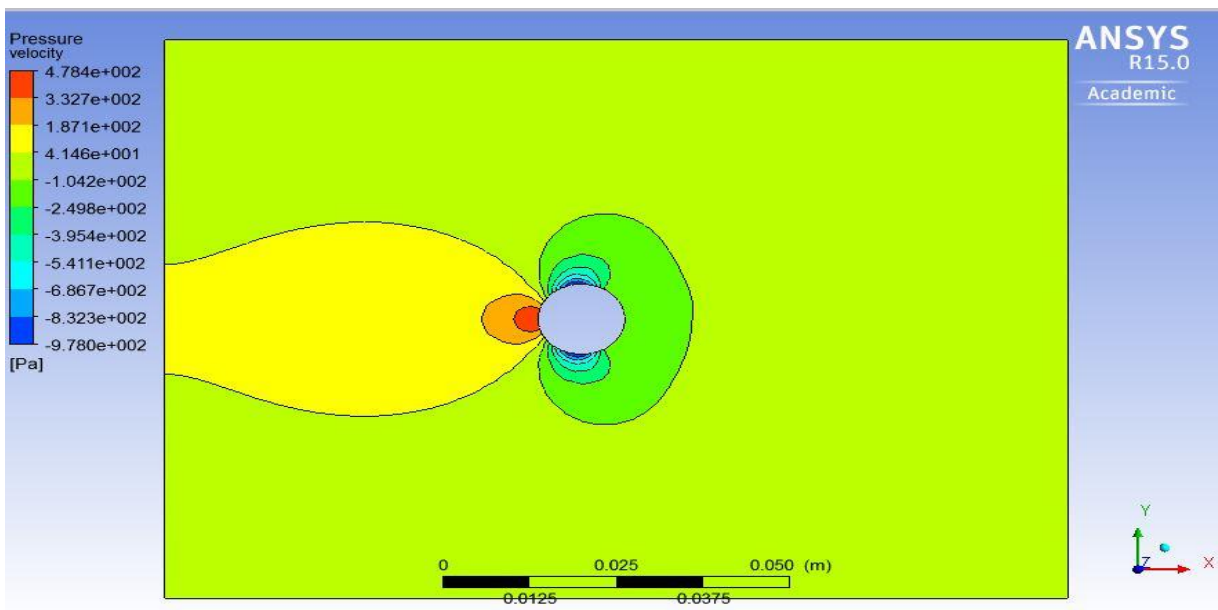


**Fig.6.15: Pressure Contour for R=6.25mm**

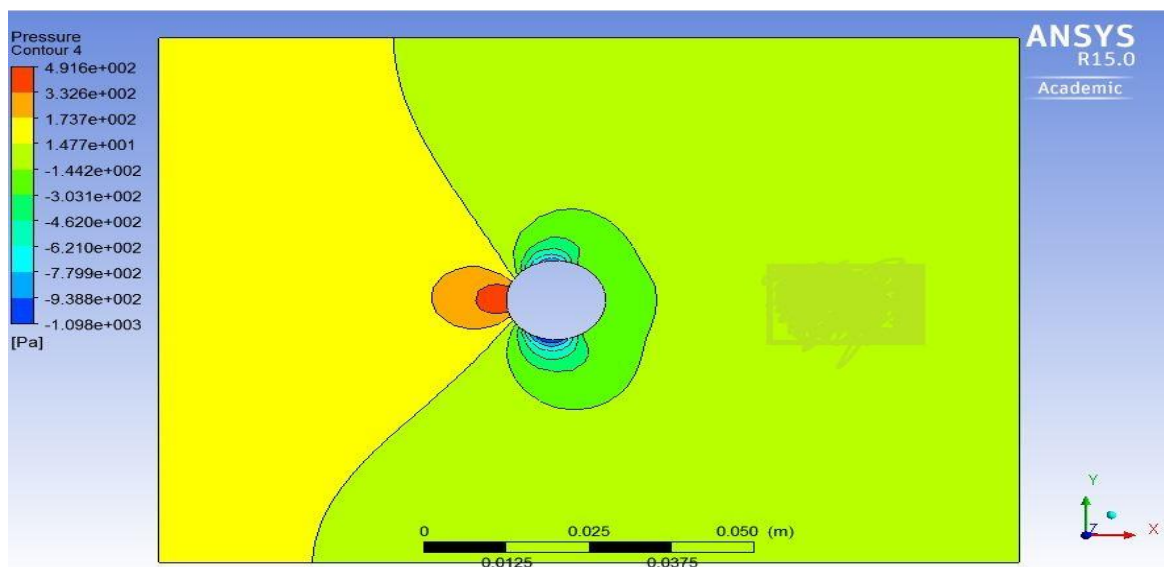


**Fig.6.16: Pressure Contour for R=7.5mm**

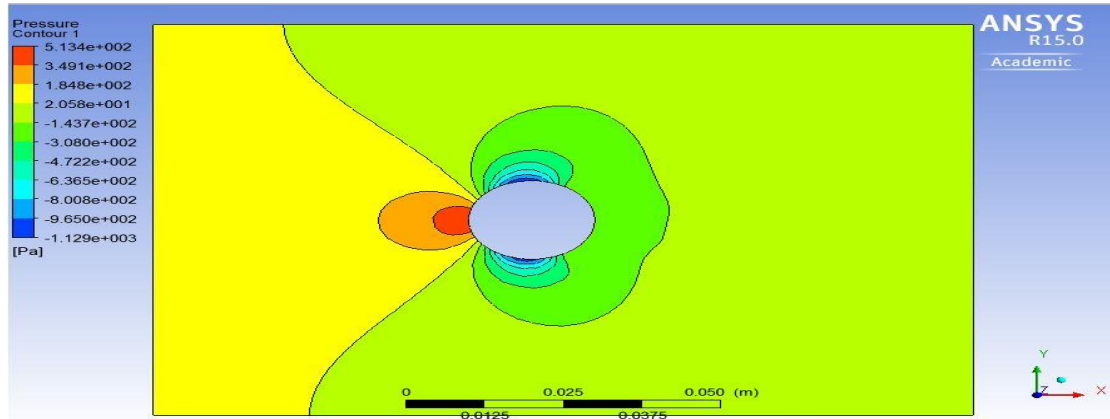


**Fig.6.17: Pressure Contour for R=10mm**

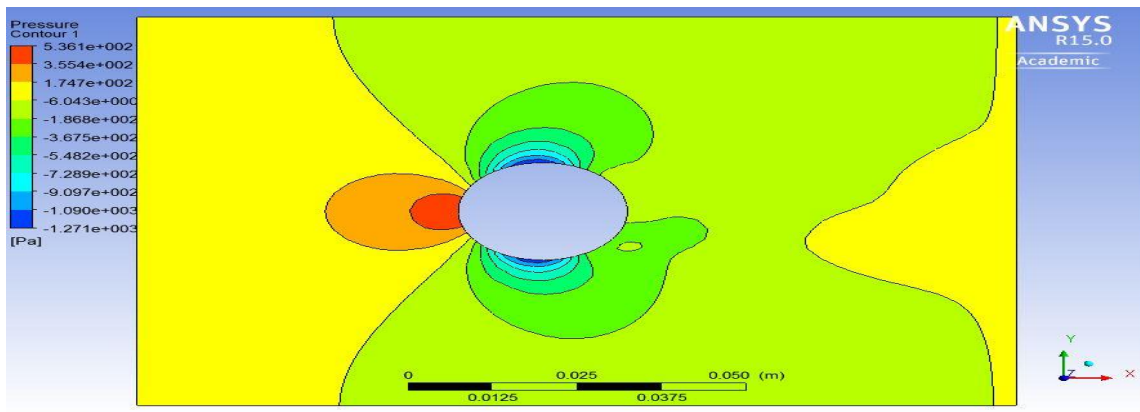


**Fig.6.18: Pressure Contour for R=12.5mm**

*b) Velocity Contour*

The corresponding velocity contour are presented for the constant velocity of 22.6 m/s of varying radius of the cylinder.

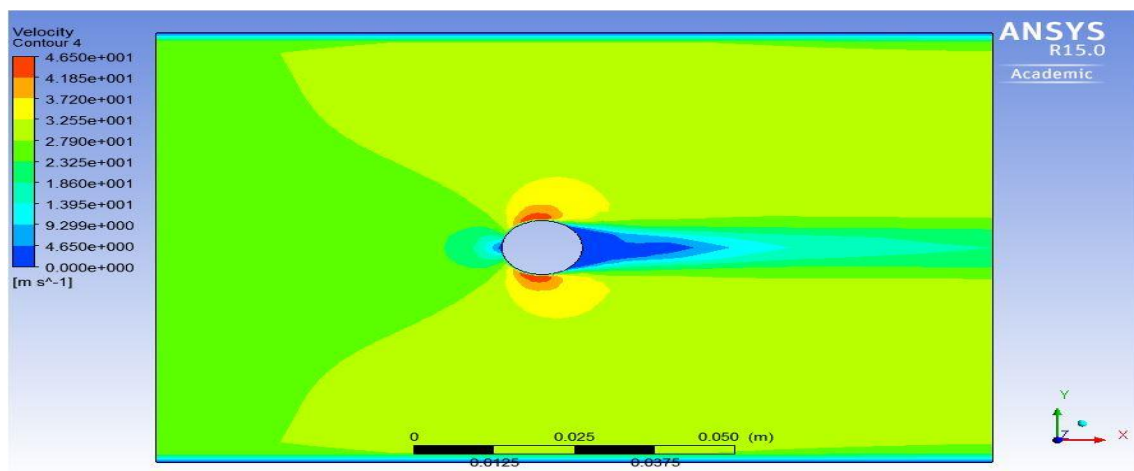


**Fig.6.19: Velocity Contour for R=6.25mm**

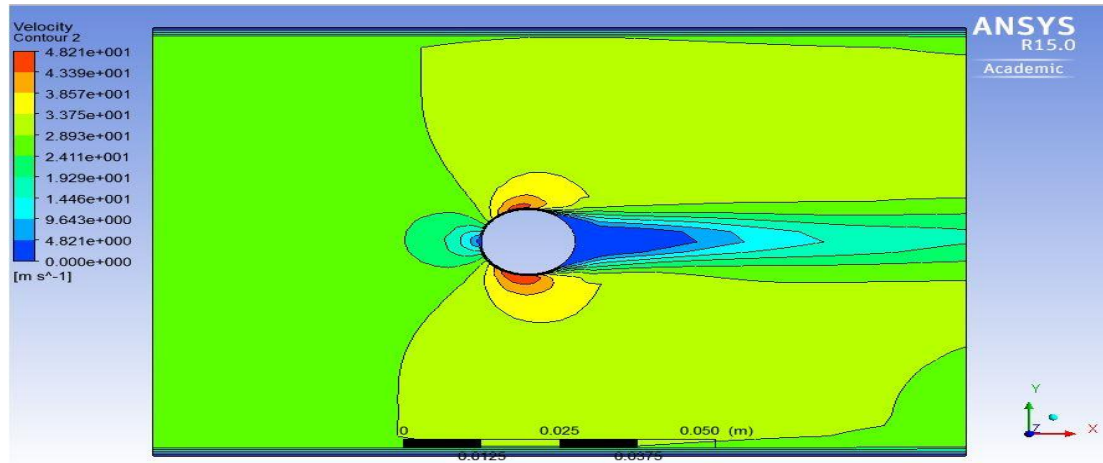


Fig.6.20: Velocity Contour for R=7.5mm

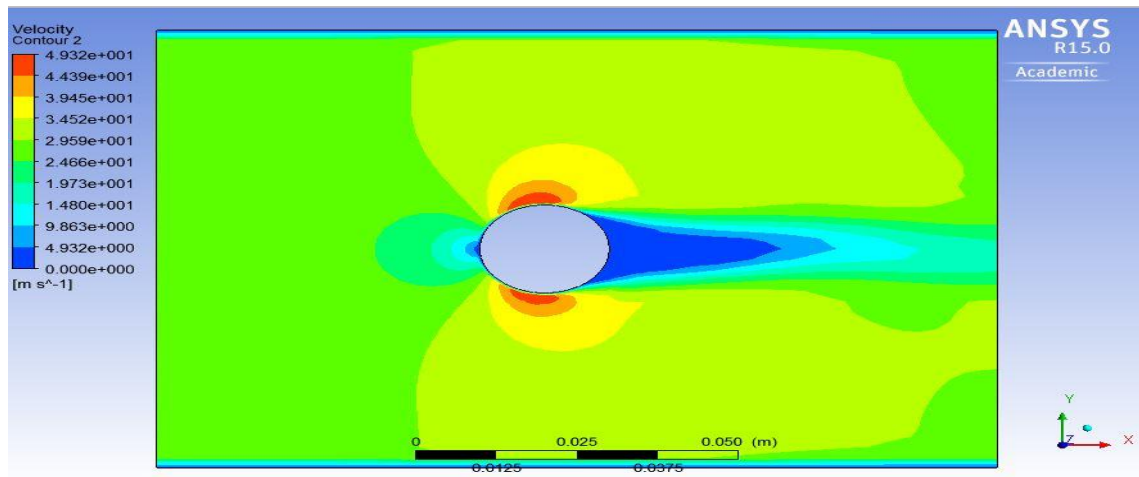


Fig.6.21: Velocity Contour for R=10mm

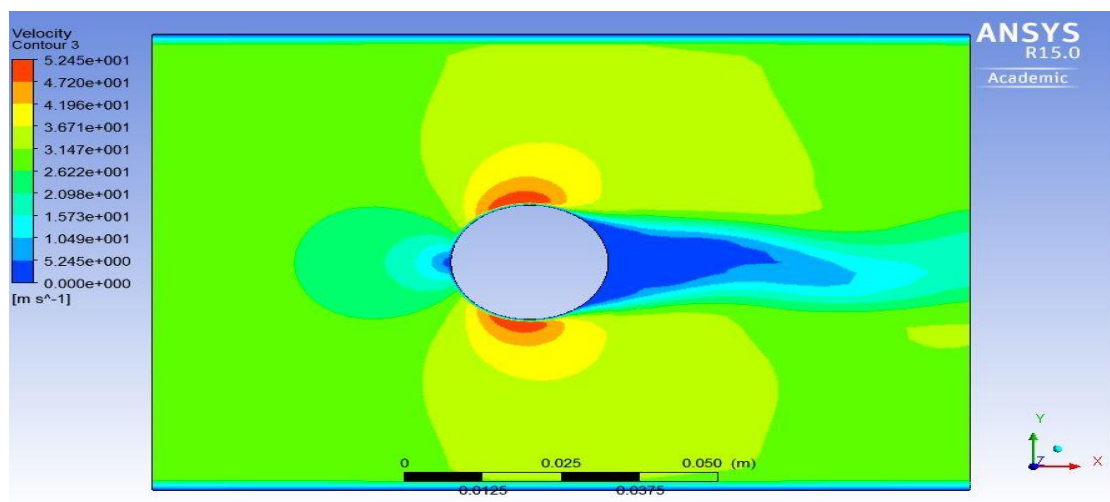


Fig.6.22: Velocity Contour for R=12.5mm

## DISCUSSION OF RESULTS

In all the above figure of velocity contour, the velocity on the upper surface of the cylinder is found to be maximum and low velocity at rear of the cylinder due to formation of wake. The wake behind the cylinder are clearly visible on the vector plot presented next.

### c) Velocity Magnitude Vector Plot

The vector plot in ANSYS, shows the magnitude and direction of the velocity when the fluid pass the cylinder. The velocity profile around the cylinder can be noticed in the vector plot.

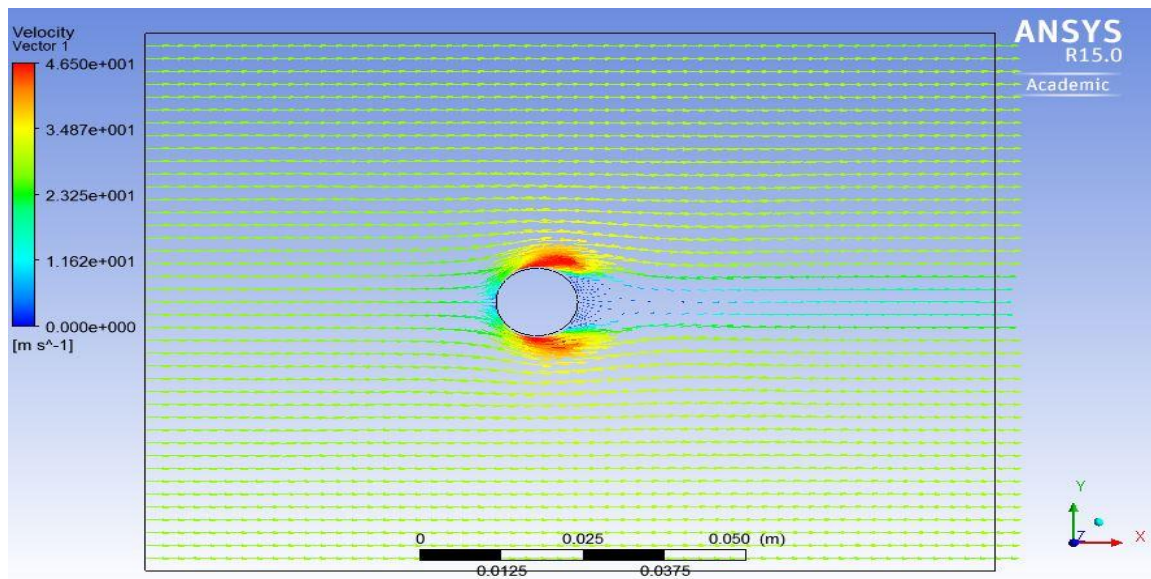


**Fig.6.23: Velocity Vector for R=6.25mm**

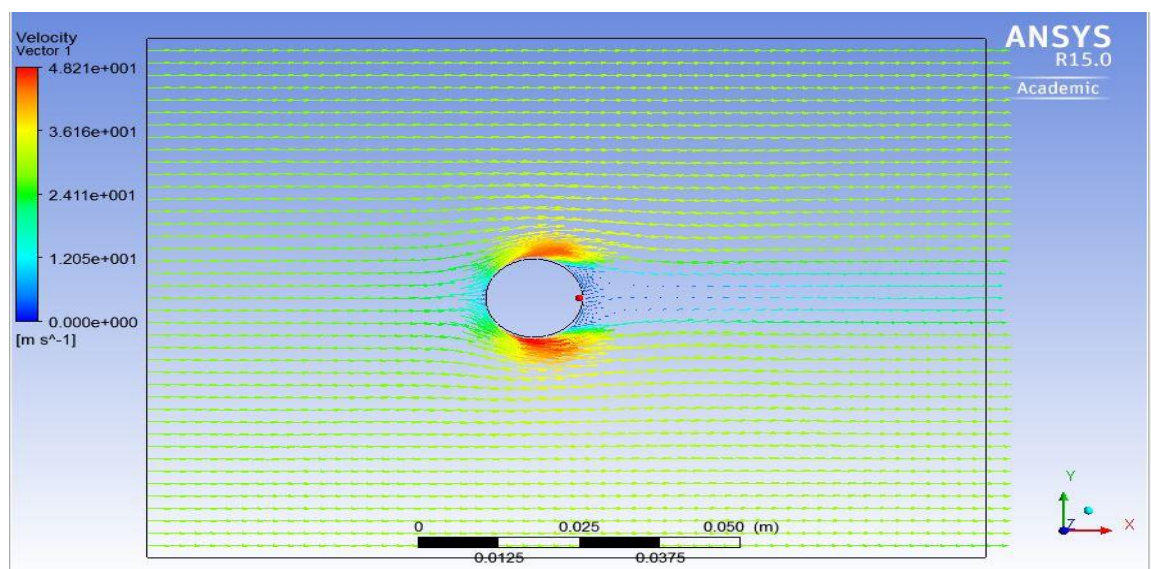
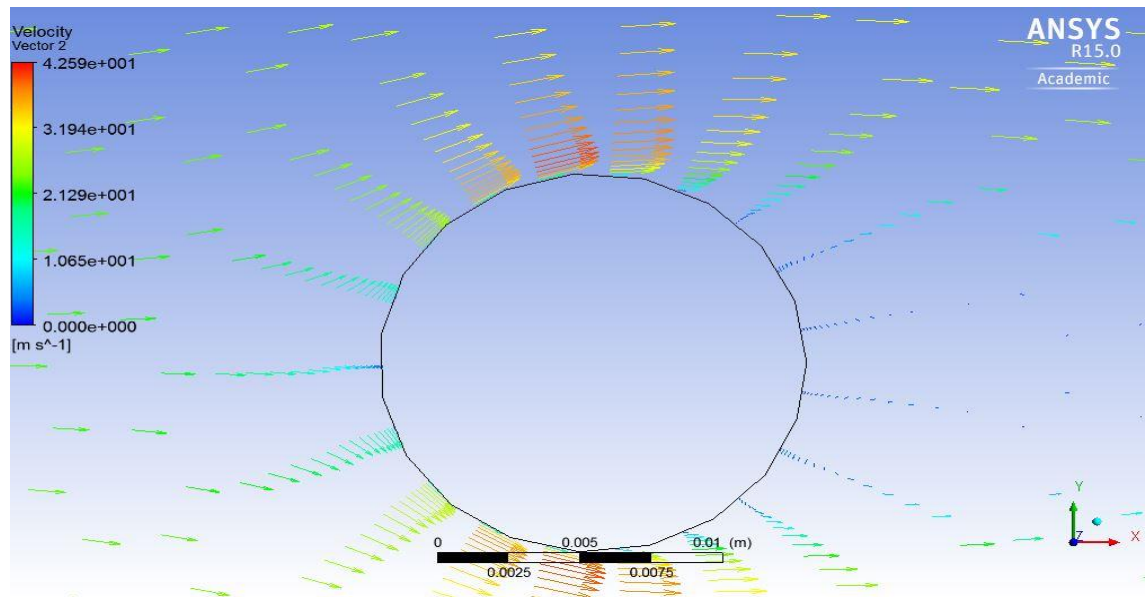
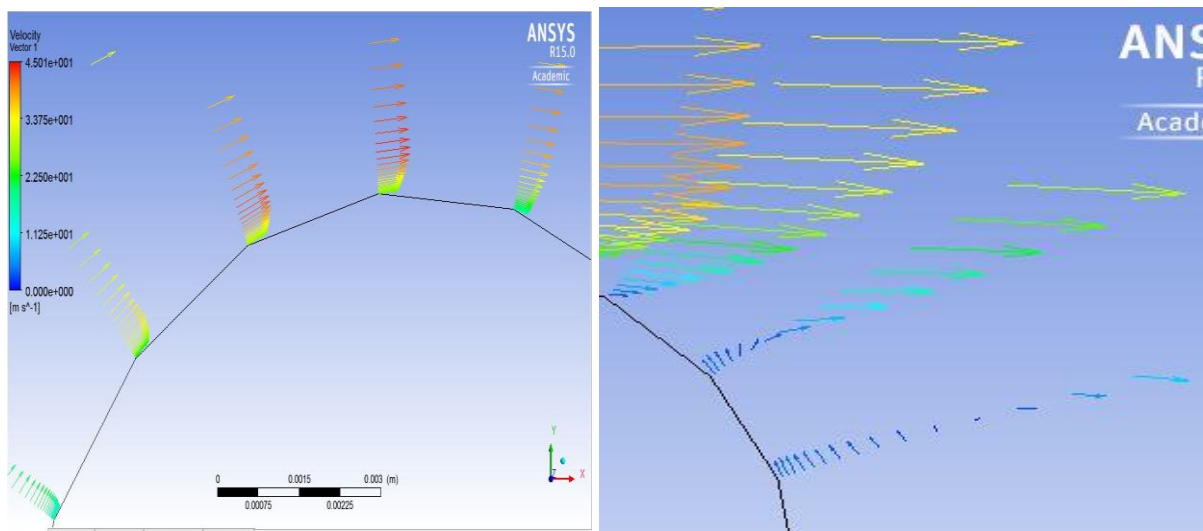


**Fig.6.24: Velocity Vector for R=7.5mm**



(a)



(b)

(c)

**Fig.6.25: (a) Close View of Velocity Vector around the Cylinder; (B) Velocity Profile and (C) Flow Separation**

The closer look over the vector plot provides better visualization and understanding of flow around the cylinder. The flow separation take place at the rear or tail of the cylinder.

### 6.3 Experiment Results

With the help of Pressure distribution technique, the pressure coefficient are found and pressure distribution over the cylinder observed.



### DISCUSSION OF RESULTS

The coefficient of drag over the cylinder is calculated from the pressure coefficient as mentioned in the previous chapter. The coefficient of pressure is plotted against the angle of rotation of cylinder. Integrating area under this curve gives the  $C_D$ . The plot of pressure coefficient for different surface roughness is presented.

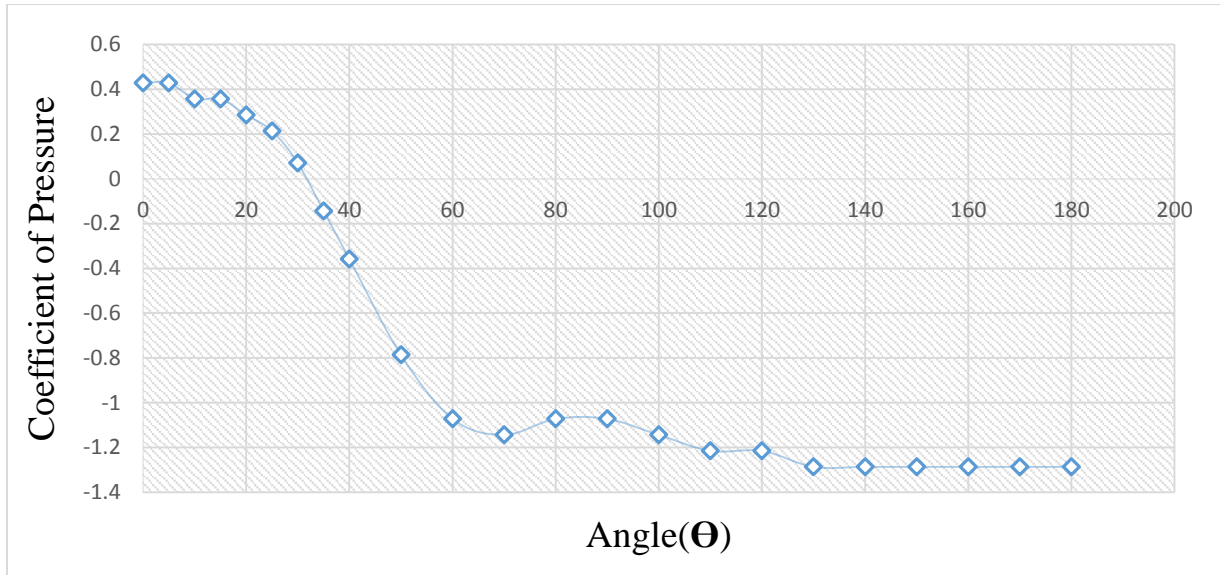


Fig.6.26: Pressure coefficient for R=7.5mm; k=348μm

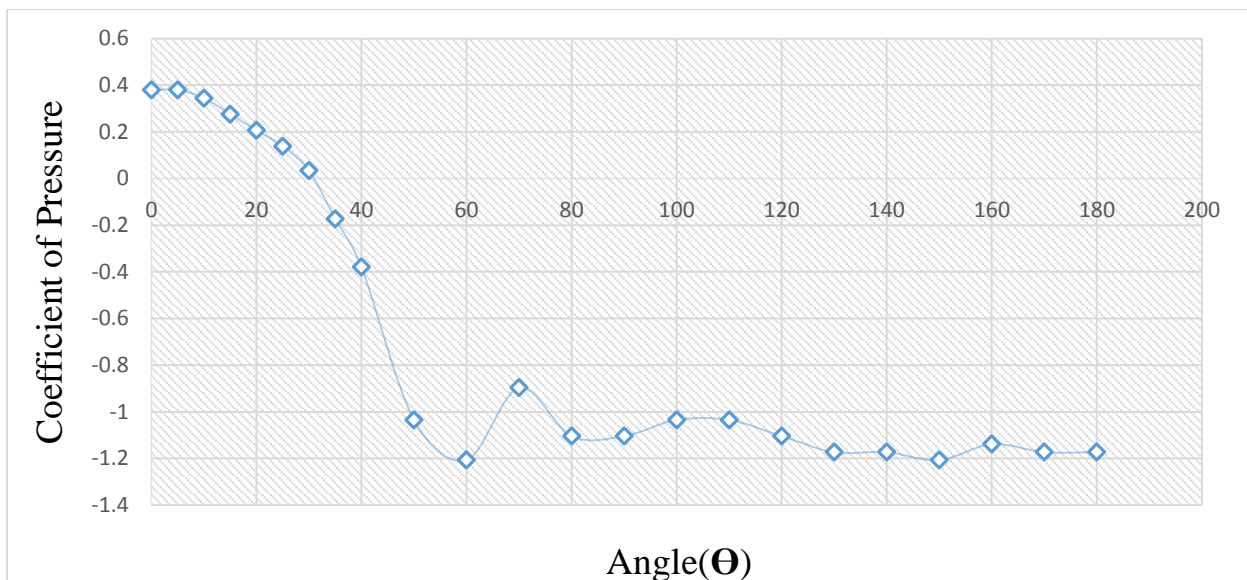


Fig.6.27: Pressure coefficient for R=7.5mm; k=265μm

The pressure coefficient plot describe the flow to be separated at  $80^{\circ}$  nearly which is similar to the value obtained by numerical study. All the plot has not been shown here.

### 6.4 Development of Correlation

The relationship between the drag force and dynamic pressure with the coefficient of drag is well known. The drag coefficient is directly proportional to drag force and inversely proportional to the dynamic pressure. The drag force is affected by the application of roughness and dynamic pressure directly depends on flow velocity  $V$ , fluid density  $\rho$  and area  $A$ , consequently these parameters ( $A$ ,  $V$ ,  $\rho$  and  $k_s$ ) brings great change in the value of drag coefficient. For the current work, Regression and Dimensional Analysis is implemented. The variable used for the dimensional analysis are independent and dependent variable. These variable tested on experiments are the flow velocity, surface roughness, and cylinder's diameter. The experimental value are collected for these varying parameter to find the drag force. All these parameter are being dimensionalised by analysing the dimension.

The drag force is given as  $F_D = 0.5\rho AV^2 C_D$ ; Thus the drag is the function of velocity ( $V$ ), diameter ( $D$ ), and roughness ( $k$ ).

$$F_D = f(V, D, k)$$

and dimensional term are given as:

$$F_D = C(V^{n_1})(D^{n_2})(k^{n_3})$$

The different plot are made according to the drag variation for various variables i.e.  $V$ ,  $D$ ,  $k$ , and there exponent is noted down. These plots are presented in following figure.

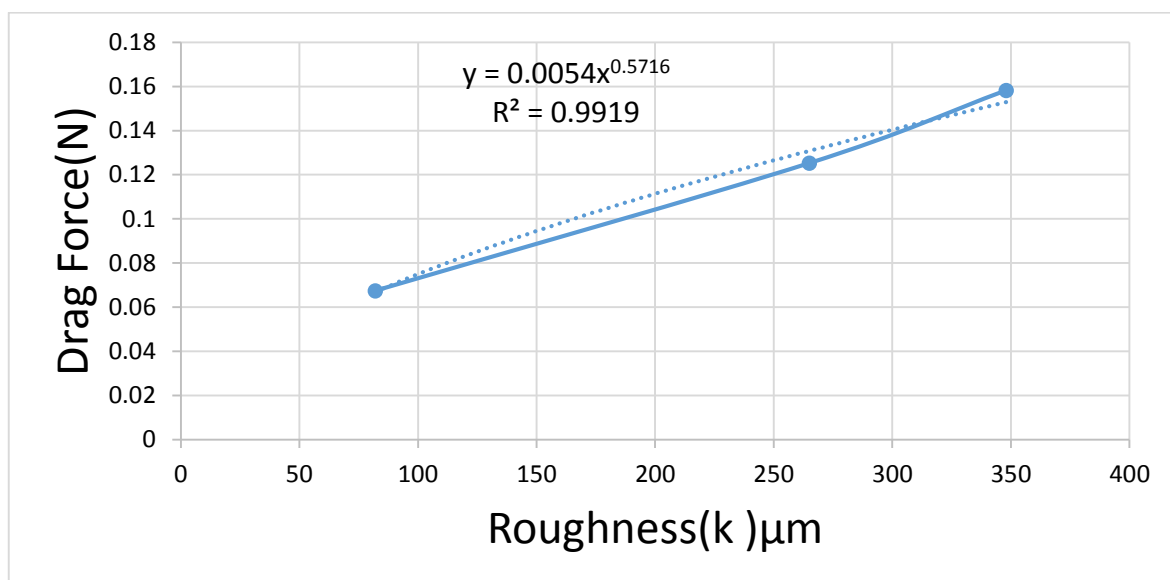


**Fig. 6.28: Drag force against varying roughness**

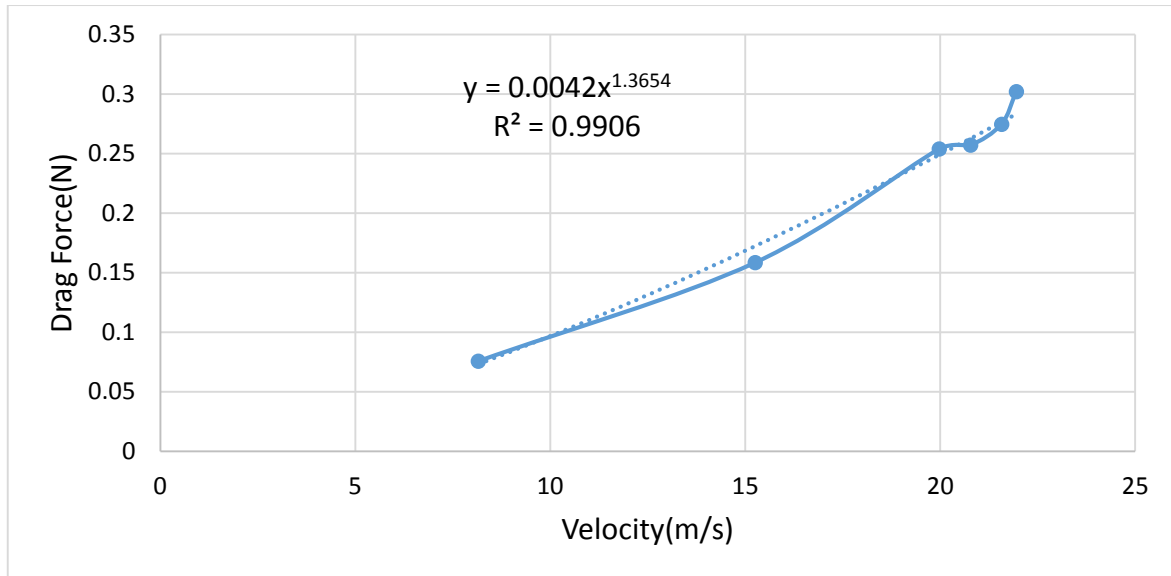


**Fig. 6.29: Drag force against varying flow velocity**

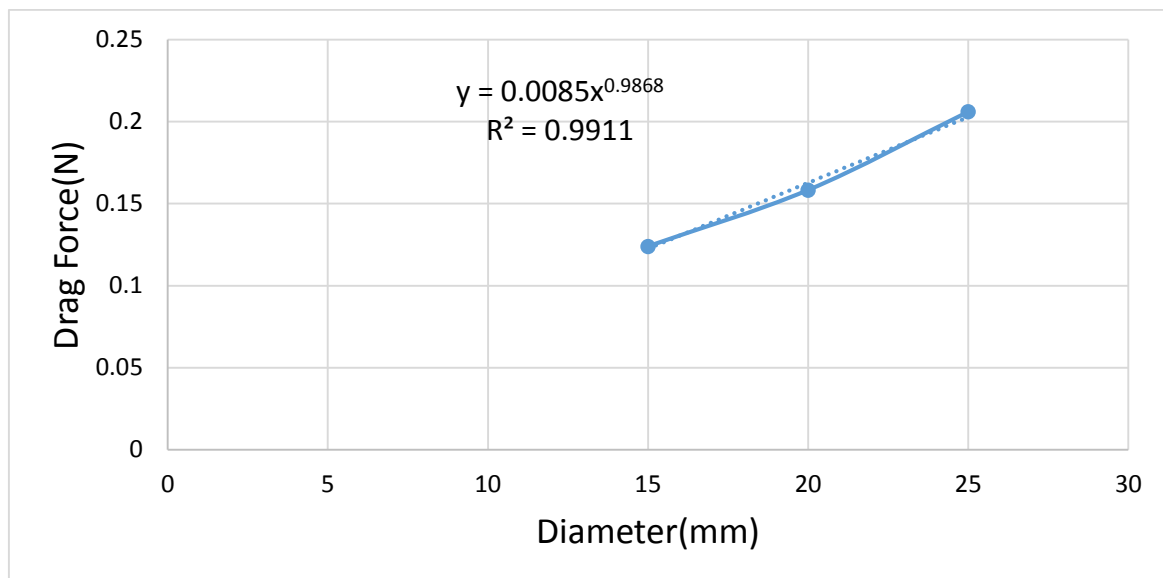


**Fig. 6.30: Drag force against varying diameter**

The exponential value are recorded as:

$$n_1=0.9919,$$

$$n_2=0.9906,$$

$$n_3=0.9911,$$

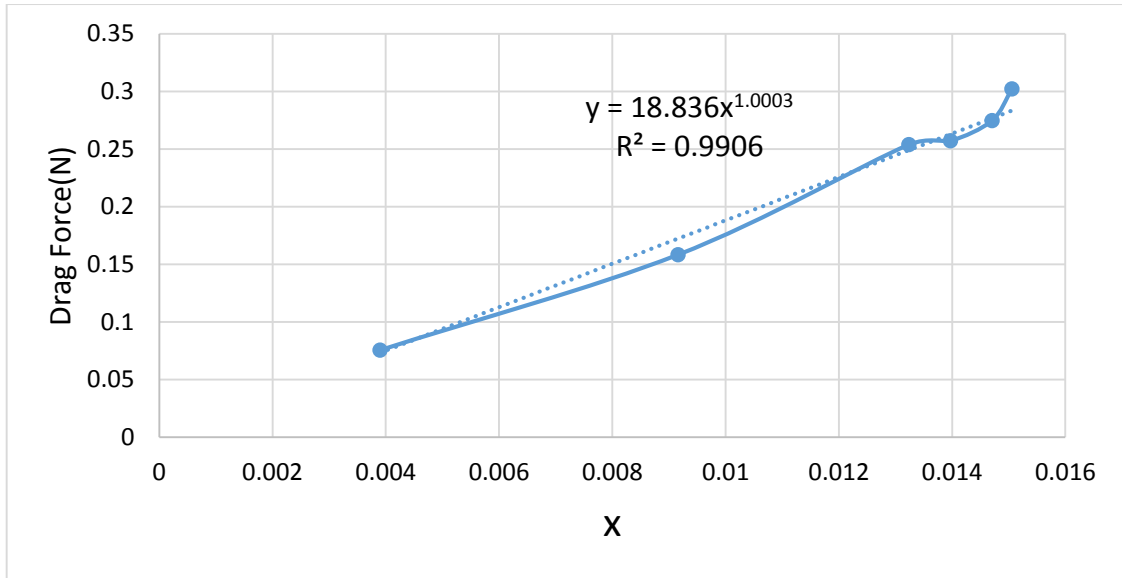


**Fig.6.31 The relationship between Drag force and x**

The exponential term are used to find the X, which is given as:  $X = (V)^{n_1}(D)^{n_2}(k)^{n_3}$  and the graph has been drawn for the drag force and X.

$$y = 18.836x^{1.0003}$$

$$R^2 = 0.9906$$

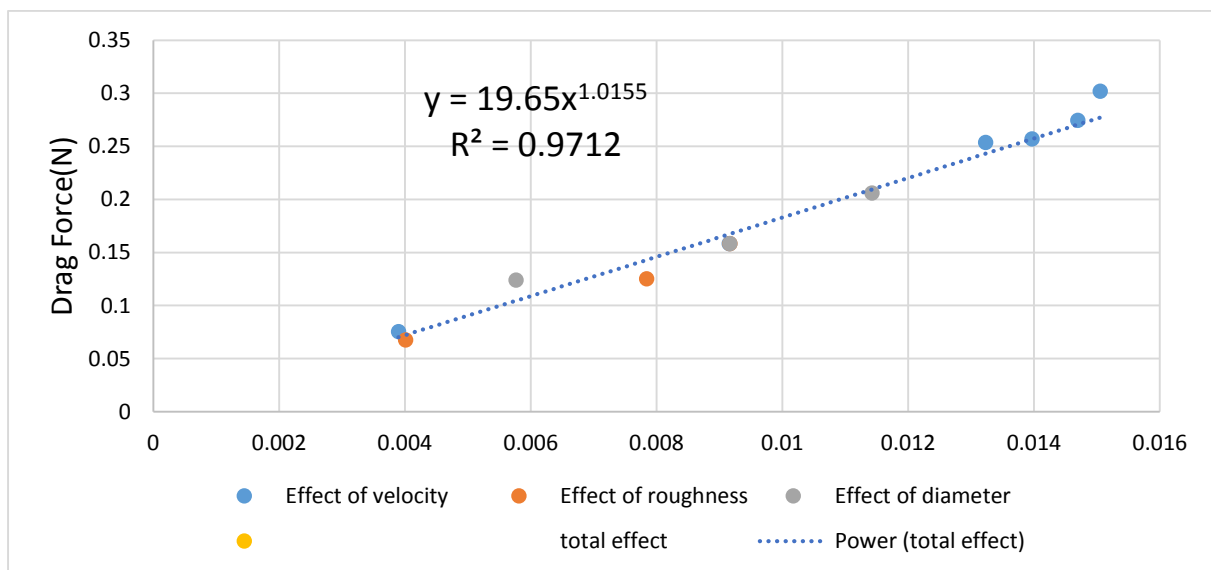


**Fig.6.32: Final correlation**

The final correlation plot is given in the figure 6.31 showing the combine effect of diameter, roughness and velocity. With the help of correlation established, the drag force is calculated or predicted and compared with the value of ANSYS and experiment, which is presented in the form of graph.

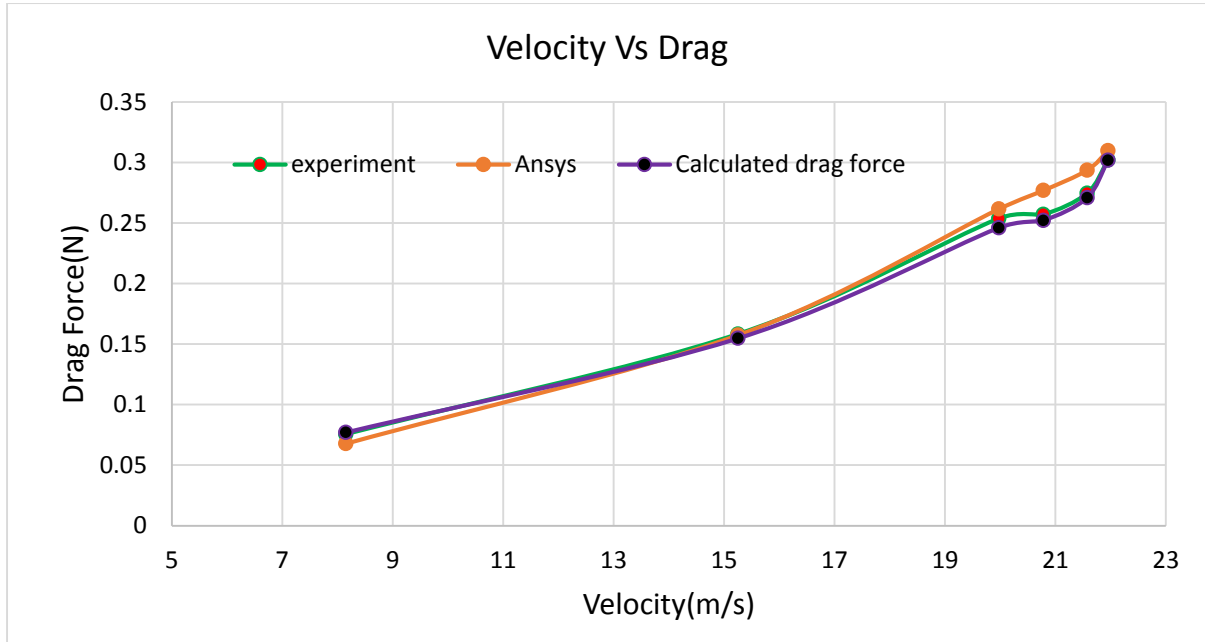


**Fig.6.33: Comparison plot for varying velocity**

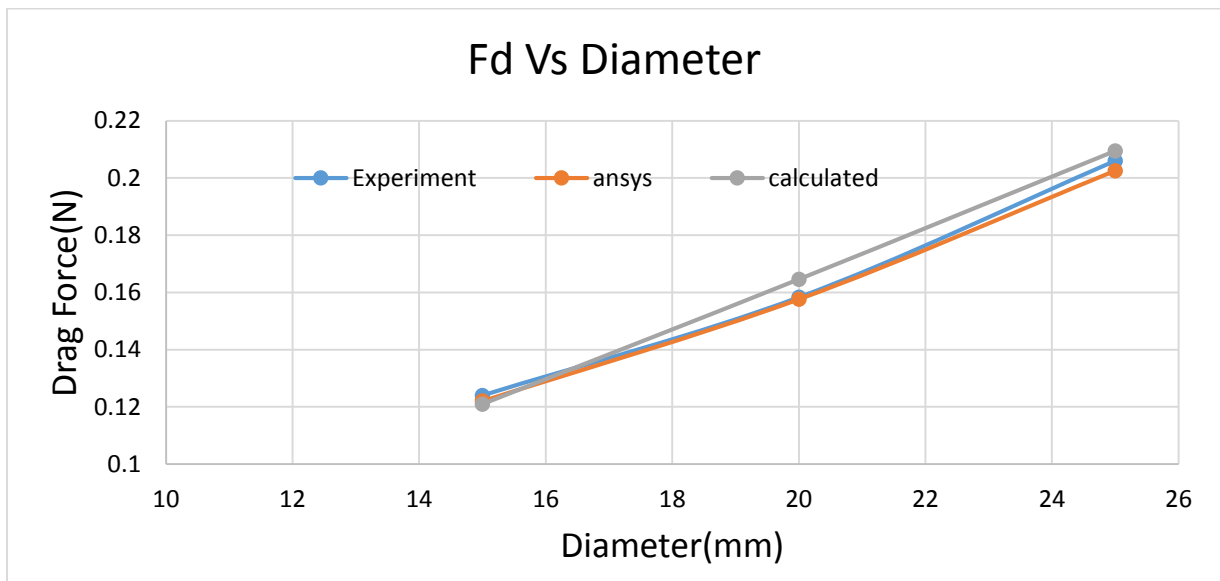


**Fig.6.34: Comparison plot for varying Diameter**

The drag force obtained from all method are quite satisfying with minimum error of 3.2% and graph plotted in between them are good.

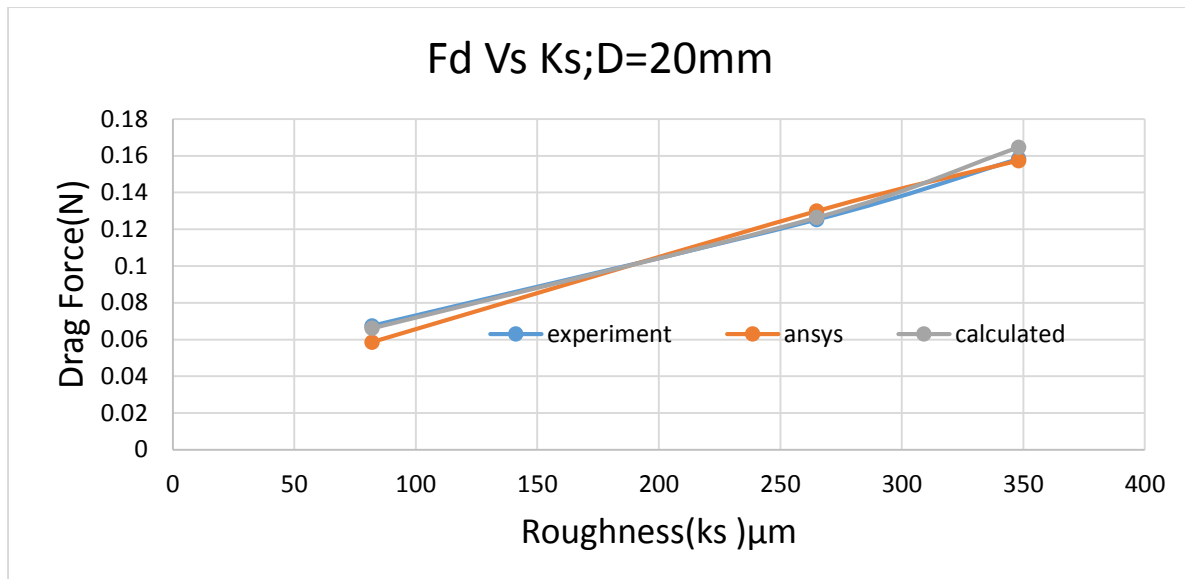


**Fig.6.35: Comparison plot for varying Roughness**

The results obtained from the numerical methods are quite easy in conducting and time saving. In comparison to the experiment it is cost effective i.e. no extra cost required for the modification of model.

## CHAPTER 7

### CONCLUSIONS AND FUTURE SCOPE

---

#### 7.1 GENERAL

The study holds the fine literature writing and good work of analysis. The drag force calculated by ANSYS software, experimental method has achieved the agreeable and satisfied solution by ensuring with the predicted data obtained from the developed correlation. This chapter describe the short view on the drag variation and its dependence on the flow and physical property of cylinder.

#### 7.2 Drag Force

The nature of drag force is listed as it react to the different parameter considering the fluid properties and geometric properties of the cylinder.

- ✓ When the area of the cylinder is increased by increasing the diameter or length, the drag force found to be increasing.
- ✓ With the increase in velocity of the fluid flow, the drag increases but its coefficient gets reduced.
- ✓ In comparison to the smooth cylinder i.e. no roughness height and the cylinder having any roughness height, the drag force on the smooth cylinder is more.
- ✓ The cylinder having increase in the roughness by increasing the previous rough surface, the drag force in such was seen to be increased.
- ✓ The drag force gets increased when the  $Re$  value is increased, but the  $C_D$  drops down.
- ✓ The drag coefficient  $C_D$  is found to be increase for the transition range.
- ✓ The velocity profile observed explains the formation of boundary layer over the cylinder surface which force the flow to be turbulent, reducing the pressure force and thus the drag gets decreased on application of roughness.
- ✓ The flow separation occurred as the consequence of distributed pressure over the cylinder was found at an angle  $70^\circ - 80^\circ$ .
- ✓ At a uniform Reynolds No. the drag force is increased and coefficient of drag is reduced for the increase in relative roughness value.
- ✓ All the method employed are compared with each other and found to good and acceptable value with error percentage of 3%.

### 7.3 Scope of the Study

This is an important study having many application in pipe flow; aerodynamic study of vehicle, buildings, high towers, and the underwater vehicle e.g. submarine.

- ✓ The investigated results can be compared with the experimentation done in wind tunnel.
- ✓ Different types of model differ in shapes can tested. The shapes can be square, triangle, elliptical, concave or convex etc.
- ✓ The hydrodynamic force acting on the body submerged in the water can be studied and drag imposed on the body could be determined.
- ✓ The numerical study can be done on the turbine.



## REFERENCES

---

- ✓ Achenbach, E., and E. Heinecke. "On vortex shedding from smooth and rough cylinders in the range of Reynolds numbers  $6 \times 10^3$  to  $5 \times 10^6$ ." *Journal of fluid mechanics* 109 (1981): 239-251.
- ✓ Akoz, M. S., & Kirkgoz, M. S. (2009). Numerical and experimental analyses of the flow around a horizontal wall-mounted circular cylinder. *Transactions of the Canadian Society for Mechanical Engineering*, 33(2), 189-215.
- ✓ Alam, M. M., Moriya, M., & Sakamoto, H. (2003). Aerodynamic characteristics of two side-by-side circular cylinders and application of wavelet analysis on the switching phenomenon. *Journal of Fluids and Structures*, 18(3), 325-346.
- ✓ Alridge, T. R., Piper, B. S., & Hunt, J. C. R. (1978). The drag coefficient of finite-aspect-ratio perforated circular cylinders. *Journal of Wind Engineering and Industrial Aerodynamics*, 3(4), 251-257.
- ✓ Bearman, P. W., & Harvey, J. K. (1993). Control of circular cylinder flow by the use of dimples. *AIAA journal*, 31(10), 1753-1756.
- ✓ Bergmann, M., Cordier, L., & Brancher, J. P. (2007). Drag minimization of the cylinder wake by trust-region proper orthogonal decomposition. In *Active Flow Control* (pp. 309-324). Springer Berlin Heidelberg.
- ✓ Bouak, F., & Lemay, J. (2001). Use of the wake of a small cylinder to control unsteady loads on a circular cylinder. *Journal of visualization*, 4(1), 61-72.
- ✓ Butt, U., & Egbers, C. (2013). Aerodynamic Characteristics of Flow over Circular Cylinders with Patterned Surface. *J. Materials, Mechanics, Manufacturing*, 1(2).

- ✓ Catalano, P., Wang, M., Iaccarino, G., & Moin, P. (2003). Numerical simulation of the flow around a circular cylinder at high Reynolds numbers. *International Journal of Heat and Fluid Flow*, 24(4), 463-469.
- ✓ D'auteuil, A., Larose, G. L., & Zan, S. J. (2012). Wind turbulence in speed skating: measurement, simulation and its effect on aerodynamic drag. *Journal of Wind Engineering and Industrial Aerodynamics*, 104, 585-593.
- ✓ Grosche, F. R., & Meier, G. E. A. (2001). Research at DLR Göttingen on bluff body aerodynamics, drag reduction by wake ventilation and active flow control. *Journal of Wind Engineering and Industrial Aerodynamics*, 89(14), 1201-1218.
- ✓ Hodžić, N., & Begagić, R. (2011). EXPERIMENTAL INVESTIGATION OF BOUNDARY LAYER SEPARATION INFLUENCE OF PRESSURE DISTRIBUTION ON CYLINDER SURFACE IN WIND TUNNEL ARMFIELD C15-10. *Trends in the Development of Machinery and Associated Technology*.
- ✓ Islam, T., & Hassan, S. R. (2013). Experimental and Numerical Investigation of Flow over a Cylinder at Reynolds Number 10 5. *Journal of Modern Science and Technology*, 1(1), 52-60.
- ✓ Jones, D. A., & Clarke, D. B. (2008). Simulation of the Flow Past a Sphere using the Fluent Code.
- ✓ Lee, S. J., Lee, S. I., & Park, C. W. (2004). Reducing the drag on a circular cylinder by upstream installation of a small control rod. *Fluid dynamics research*, 34(4), 233-250.
- ✓ Ling, G. P., & Shih, T. M. (1999). Numerical study on the vortex motion patterns around a rotating circular cylinder and their critical characters. *International journal for numerical methods in fluids*, 29(2), 229-248.
- ✓ Lyotard, N., Shew, W. L., Bocquet, L., & Pinton, J. F. (2007). Polymer and surface roughness effects on the drag crisis for falling spheres. *The European Physical Journal B-*



## REFERENCE

*Condensed Matter and Complex Systems*, 60(4), 469-476.

- ✓ Mahesh, K., Constantinescu, G., & Moin, P. (2004). A numerical method for large-eddy simulation in complex geometries. *Journal of Computational Physics*, 197(1), 215-240.
- ✓ Mashud, M., Islam, M. S., Bari, G. S., & Islam, M. R. (2010). Reduction of Drag Force of a Cylinder by Attaching Cylindrical Rings. Proceedings of the 13th Asian Congress of Fluid Mechanics, (2010), Dhaka, Bangladesh.
- ✓ Merrick, Ryan, and Girma Bitsuamlak. (1982). Control of flow around a circular cylinder by the use of surface roughness: A computational and experimental approach. *Journal of Fluid Mechanics*, 123, 363-378.
- ✓ Mittal, R., & Balachandar, S. (1995). Effect of three-dimensionality on the lift and drag of nominally two-dimensional cylinders. *Physics of Fluids (1994-present)*, 7(8), 1841-1865.
- ✓ Mittal, S., & Raghuvanshi, A. (2001). Control of vortex shedding behind circular cylinder for flows at low Reynolds numbers. *International Journal for Numerical Methods in Fluids*, 35(4), 421-447.
- ✓ Mittal, S., & Singh, S. (2005). Vortex-induced vibrations at subcritical Re. *Journal of Fluid Mechanics*, 534, 185-194.
- ✓ Monalisa Mallick and A. Kumar (2014), "Study on Drag Coefficient for the Flow Past a Cylinder" *International Journal of Civil Engineering Research*. Volume 5, pp. 301-306
- ✓ Monalisa Mallick and A. Kumar (2014), "Experimental Investigation of Flow past a Rough Surfaced Cylinder" *International Journal of Engineering Research and Applications*.
- ✓ Nils P. van Hinsberg (2014), "The Reynolds number effect from subcritical to high trans-critical on steady and unsteady loading on a rough circular cylinder" *International Conference on Structural Dynamics*. 978-972-752-165-4
- ✓ Njock Libii, J. (2010). Using wind tunnel tests to study pressure distributions around a

bluff body: the case of a circular cylinder. *Transactions on Engineering and Technology Education*, 8(3).

- ✓ Protas, B., & Wesfreid, J. E. (2002). Drag force in the open-loop control of the cylinder wake in the laminar regime. *Physics of Fluids (1994-present)*, 14(2), 810-826.
- ✓ Richter, A., & Nikrityuk, P. A. (2012). Drag forces and heat transfer coefficients for spherical, cuboidal and ellipsoidal particles in cross flow at sub-critical Reynolds numbers. *International Journal of Heat and Mass Transfer*, 55(4), 1343-1354.
- ✓ Shao, Y., & Yang, Y. (2005). A scheme for drag partition over rough surfaces. *Atmospheric Environment*, 39(38), 7351-7361.
- ✓ Shih, W. C. L., Wang, C., Coles, D., & Roshko, A. (1993). Experiments on flow past rough circular cylinders at large Reynolds numbers. *Journal of Wind Engineering and Industrial Aerodynamics*, 49(1), 351-368.
- ✓ Singh, S. P., & Mittal, S. (2005). Flow past a cylinder: shear layer instability and drag crisis. *International Journal for Numerical Methods in Fluids*, 47(1), 75-98.
- ✓ Sørensen, N. N., Bechmann, A., & Zahle, F. (2011). 3D CFD computations of transitional flows using DES and a correlation based transition model. *Wind Energy*, 14(1), 77-90.
- ✓ Tamayol, A., Yeom, J., Akbari, M., & Bahrami, M. (2013). Low Reynolds number flows across ordered arrays of micro-cylinders embedded in a rectangular micro/minichannel. *International Journal of Heat and Mass Transfer*, 58(1), 420-426.
- ✓ Timmer, W. A., & Schaffarczyk, A. P. (2004). The effect of roughness at high Reynolds numbers on the performance of aerofoil DU 97-W-300Mod. *Wind Energy*, 7(4), 295-307.
- ✓ Triyogi, Y., D. Suprayogi, and E. Spirda. (2009). "Reducing the drag on a circular cylinder by upstream installation of an I-type bluff body as passive control. "Proceedings of the Institution of Mechanical Engineers, Part C: Journal of Mechanical Engineering Science 223.10: 2291-2296.



## REFERENCE

- ✓ Tsutsui, T., & Igarashi, T. (2002). Drag reduction of a circular cylinder in an air-stream. *Journal of Wind Engineering and Industrial Aerodynamics*, 90(4), 527-541.
- ✓ Wang, Y. X., Lu, X. Y., & Zhuang, L. X. (2004). Numerical analysis of the rotating viscous flow approaching a solid sphere. *International journal for numerical methods in fluids*, 44(8), 905-925. Roshko, A. (1961). Experiments on the flow past a circular cylinder at very high Reynolds number. *Journal of Fluid Mechanics*, 10(03), 345-356.
- ✓ Williamson, C. H. (1996). Vortex dynamics in the cylinder wake. *Annual review of fluid mechanics*, 28(1), 477-539.
- ✓ Xu, C. Y., Chen, L. W., & Lu, X. Y. (2010). Large-eddy simulation of the compressible flow past a wavy cylinder. *Journal of Fluid Mechanics*, 665, 238-273.
- ✓ Zakharenkov, M. N. (1997). Unsteady detached separation from a circular cylinder performing rotational oscillations in a uniform viscous incompressible flow. *International journal for numerical methods in fluids*, 25(2), 125-142.
- ✓ Zheng, Z. C., & Zhang, N. (2008). Frequency effects on lift and drag for flow past an oscillating cylinder. *Journal of Fluids and Structures*, 24(3), 382-399.